

1 **Effects of elevated CO<sub>2</sub> and temperature on phytoplankton community**  
2 **biomass, species composition and photosynthesis during an**  
3 **experimentally induced autumn bloom in the Western English**  
4 **Channel**

5 Matthew Keys<sup>1,2</sup>, Gavin Tilstone<sup>1\*</sup>, Helen S. Findlay<sup>1</sup>, Claire E. Widdicombe<sup>1</sup> and Tracy Lawson<sup>2</sup>.

6 <sup>1</sup> Plymouth Marine Laboratory, Prospect Place, The Hoe, Plymouth, PL1 3DH, UK.

7 <sup>2</sup> University of Essex, Wivenhoe Park, Colchester, CO4 3SQ, UK.

8 *Correspondence to:* G. Tilstone (ghti@pml.ac.uk)

9

10 **Abstract**

11 The combined effects of elevated pCO<sub>2</sub> and temperature were investigated during an  
12 experimentally induced autumn phytoplankton bloom *in vitro* sampled from the Western  
13 English Channel (WEC). A full factorial 36-day microcosm experiment was conducted under  
14 year 2100 predicted temperature (+ 4.5 °C) and pCO<sub>2</sub> levels (800 µatm). Over the experimental  
15 period total phytoplankton biomass was significantly influenced by elevated pCO<sub>2</sub>. At the end of  
16 the experiment, biomass increased 6.5-fold under elevated pCO<sub>2</sub> and 4.6-fold under elevated  
17 temperature relative to the ambient control. By contrast, the combined influence of elevated  
18 pCO<sub>2</sub> and temperature had little effect on biomass relative to the control. Throughout the  
19 experiment in all treatments and in the control, the phytoplankton community structure shifted  
20 from dinoflagellates to nanophytoplankton . At the end of the experiment, under elevated pCO<sub>2</sub>  
21 nanophytoplankton contributed 90% of community biomass and was dominated by *Phaeocystis*  
22 spp.. Under elevated temperature, nanophytoplankton comprised 85% of the community  
23 biomass and was dominated by smaller nano-flagellates. In the control, larger nano-flagellates  
24 dominated whilst the smallest nanophytoplankton contribution was observed under combined  
25 elevated pCO<sub>2</sub> and temperature (~40 %). Under elevated pCO<sub>2</sub>, temperature and in the control,  
26 there was a significant decrease in dinoflagellate biomass. Under the combined effects of  
27 elevated pCO<sub>2</sub> and temperature, dinoflagellate biomass increased and was dominated by the  
28 harmful algal bloom (HAB) species, *Prorocentrum cordatum*. At the end of experiment,  
29 Chlorophyll a (Chl *a*) normalised maximum photosynthetic rates (P<sup>B<sub>m</sub></sup>) increased > 6-fold under  
30 elevated pCO<sub>2</sub> and > 3-fold under elevated temperature while no effect on P<sup>B<sub>m</sub></sup> was observed  
31 when pCO<sub>2</sub> and temperature were elevated simultaneously. The results suggest that future  
32 increases in temperature and pCO<sub>2</sub> simultaneously do not appear to influence coastal

33 phytoplankton productivity but significantly influence community composition during autumn  
34 in the WEC.

## 35 **1. Introduction**

36 Oceanic concentration of CO<sub>2</sub> has increased by ~42% over pre-industrial levels, with a  
37 continuing annual increase of ~0.4%. Current CO<sub>2</sub> level has reached ~400 μatm and has been  
38 predicted to rise to >700 μatm by the end of this century (IPCC, 2013), with estimates exceeding  
39 1000 μatm (Matear and Lenton, 2018; Raupach et al., 2007; Raven et al., 2005). With increasing  
40 atmospheric CO<sub>2</sub>, the oceans continue to absorb CO<sub>2</sub> from the atmosphere, which results in a  
41 shift in oceanic carbonate chemistry resulting in a decrease in seawater pH or 'Ocean  
42 Acidification' (OA). The projected increase in atmospheric CO<sub>2</sub> and corresponding increase in  
43 ocean uptake, is predicted to result in a decrease in global mean surface seawater pH of 0.3  
44 units below the present value of 8.1 to 7.8 (Wolf-gladrow et al., 1999). Under this scenario, the  
45 shift in dissolved inorganic carbon (DIC) equilibria has wide ranging implications for  
46 phytoplankton photosynthetic carbon fixation rates and growth (Riebesell, 2004).

47 Concurrent with OA, elevated atmospheric CO<sub>2</sub> and other climate active gases have warmed the  
48 planet by ~0.6 °C over the past 100 years (IPCC, 2007). Atmospheric temperature has been  
49 predicted to rise by a further 1.8 to 4 °C by the end of this century (Alley et al., 2007).

50 Phytoplankton metabolic activity may be accelerated by increased temperature (Eppley, 1972),  
51 which can vary depending on the phytoplankton species and their physiological  
52 requirements (Beardall et al., 2009; Boyd et al., 2013). Long-term data sets already suggest that  
53 ongoing changes in coastal phytoplankton communities are likely due to climate shifts and other  
54 anthropogenic influences (Edwards et al., 2006; Smetacek and Cloern, 2008; Widdicombe et al.,  
55 2010). The response to OA and temperature can potentially alter the community composition,  
56 community biomass and photo-physiology. Understanding how these two factors may interact,  
57 synergistically or antagonistically, is critical to our understanding and for predicting future  
58 primary productivity (Boyd and Doney, 2002; Dunne, 2014).

59 Laboratory studies of phytoplankton species in culture and studies on natural populations in  
60 the field have shown that most species exhibit sensitivity, in terms of growth and  
61 photosynthetic rates, to elevated pCO<sub>2</sub> and temperature individually. To date, only a few studies  
62 have investigated the interactive effects of these two parameters on natural populations (e.g.  
63 Coello-Camba et al., 2014; Feng et al., 2009; Gao et al., 2017; Hare et al., 2007). Most laboratory  
64 studies demonstrate variable results with species-specific responses. In the diatom  
65 *Thalassiosira weissflogii* for example, pCO<sub>2</sub> elevated to 1000 μatm and + 5 °C temperature  
66 synergistically enhanced growth, while the same conditions resulted in a reduction in growth

67 for the diatom *Dactyliosolen fragilissimus* (Taucher et al., 2015). Although there have been fewer  
68 studies on dinoflagellates, variable responses have also been reported (Errera et al., 2014; Fu et  
69 al., 2008). In natural populations, elevated pCO<sub>2</sub> has stimulated the growth of pico- and  
70 nanophytoplankton (Boras et al., 2016; Engel et al., 2008) while increased temperature has  
71 reduced their biomass (Moustaka-Gouni et al., 2016; Peter and Sommer, 2012). In a recent field  
72 study on natural phytoplankton communities, elevated temperature (+ 3°C above ambient)  
73 enhanced community biomass but the combined influence of elevated temperature and pCO<sub>2</sub>  
74 reduced the biomass (Gao et al., 2017).

75 Phytoplankton species composition, abundance and biomass has been measured since 1992 at  
76 the time-series station L4 in the western English Channel (WEC), to evaluate how global  
77 changes could drive future shifts in phytoplankton community structure and carbon  
78 biogeochemistry. At this station, sea surface temperature and pCO<sub>2</sub> reach maximum values  
79 during late summer and start to decline in autumn. During October, mean seawater  
80 temperatures at 10 m decrease from 15.39 °C (± 0.49 sd) to 14.37 °C (± 0.62 sd). Following a  
81 period of CO<sub>2</sub> oversaturation in late summer, pCO<sub>2</sub> returns to near-equilibrium at station L4 in  
82 October when mean pCO<sub>2</sub> values decrease from 455.32 µatm (± 63.92 sd) to 404.06 µatm (±  
83 38.55 sd) (Kitidis et al., 2012).

84 From a biological perspective, the autumn period at station L4 is characterised by the decline of  
85 the late summer diatom and dinoflagellate blooms (Widdicombe et al., 2010) when their  
86 biomass approaches values close to the time series minima (diatom biomass range: 6.01 (± 6.88  
87 sd) – 2.85 (± 3.28 sd) mg C m<sup>-3</sup>; dinoflagellate biomass range: 1.75 (± 3.28 sd) – 0.66 (± 1.08 sd)  
88 mg C m<sup>-3</sup>). Typically, over this period nanophytoplankton becomes numerically dominant and  
89 biomass ranges from 20.94 (± 33.25 sd) – 9.38 (± 3.31 sd) mg C m<sup>-3</sup>, though there is  
90 considerable variability in this biomass.

91 Based on the existing literature, the working hypotheses of this study are that: (1) community  
92 biomass will increase differentially under individual treatments of elevated temperature and  
93 pCO<sub>2</sub>; (2) elevated pCO<sub>2</sub> will lead to taxonomic shifts due to differences in species-specific CO<sub>2</sub>  
94 concentrating mechanisms and/or RuBisCO specificity; (3) photosynthetic carbon fixation rates  
95 will increase differentially under individual treatments of elevated temperature and pCO<sub>2</sub>; (4)  
96 elevated temperature will lead to taxonomic shifts due to species-specific thermal optima; (5)  
97 temperature and pCO<sub>2</sub> elevated simultaneously will have synergistic effects.

98 The objective of the study was therefore to investigate the combined effects of elevated pCO<sub>2</sub>  
99 and temperature on phytoplankton community structure, biomass and photosynthetic carbon

100 fixation rates during the autumn transition from diatoms and dinoflagellates to  
101 nanophytoplankton at station L4 in the WEC.

## 102 **2. Materials and methods**

### 103 **2.1 Perturbation experiment, sampling and experimental set-up**

104 Experimental seawater containing a natural phytoplankton community was sampled at station  
105 L4 (50 ° 15' N, 4 ° 13' W) on 7<sup>th</sup> October 2015 from 10 m depth (40 L). The experimental  
106 seawater was gently pre-filtered through a 200 µm Nitex mesh to remove mesozooplankton  
107 grazers, into two 20 L acid-cleaned carboys. While grazers play an important role in regulating  
108 phytoplankton community structure (e.g. Strom, 2002), our experimental goals considered only  
109 the effects of elevated temperature and pCO<sub>2</sub>, though the mesh size used does not remove  
110 microzooplankton. In addition, 320 L of seawater was collected into sixteen 20 L acid-cleaned  
111 carboys from the same depth for use as experimental media. Immediately upon return to the  
112 laboratory the media seawater was filtered through an in-line 0.2 and 0.1 µm filter (Acropak™,  
113 Pall Life Sciences) then stored in the dark at 14 °C until use. The experimental seawater was  
114 gently and thoroughly mixed and transferred in equal parts from each carboy (to ensure  
115 homogeneity) to sixteen 2.5 L borosilicate incubation bottles (4 sets of 4 replicates). The  
116 remaining experimental seawater was sampled for initial (T0) concentrations of nutrients, Chl  
117 *a*, total alkalinity, dissolved inorganic carbon, particulate organic carbon (POC) and nitrogen  
118 (PON) and was also used to characterise the starting experimental phytoplankton community.  
119 The incubation bottles were placed in an outdoor simulated in-situ incubation culture system  
120 and each set of replicates was linked to one of four 22 L reservoirs filled with the filtered  
121 seawater media. Neutral density spectrally corrected blue filters (Lee Filter no. 061) were  
122 placed between polycarbonate sheets and mounted to the top, sides and ends of the incubation  
123 system to provide ~50 % irradiance, approximating PAR measured at 10 m depth at station L4  
124 on the day of sampling prior to starting experimental incubations (see **Fig. S1**, supplementary  
125 material for time course of PAR levels during the experiment). The media was aerated with CO<sub>2</sub>  
126 free air and 5 % CO<sub>2</sub> in air precisely mixed using a mass flow controller (Bronkhorst UK  
127 Limited) and used for the microcosm dilutions as per the following experimental design: (1)  
128 control (390 µatm pCO<sub>2</sub>, 14.5 °C matching station L4 in-situ values), (2) high temperature (390  
129 µatm pCO<sub>2</sub>, 18.5 °C), (3) high pCO<sub>2</sub> (800 µatm pCO<sub>2</sub>, 14.5 °C) and (4) combination (800 µatm  
130 pCO<sub>2</sub>, 18.5 °C).

131 Initial nutrient concentrations (0.24 µM nitrate + nitrite, 0.086 µM phosphate and 2.14 µM  
132 silicate on 7<sup>th</sup> October 2015) were amended to 8 µM nitrate+nitrite and 0.5 µM phosphate.  
133 Pulses of nutrient inputs frequently occur at station L4 from August to December following

134 heavy rainfall events and subsequent riverine inputs to the system (e.g. Barnes et al., 2015). Our  
135 nutrient amendments simulated these in situ conditions and were held constant to maintain  
136 phytoplankton growth. Previous pilot studies highlighted that if these concentrations were not  
137 maintained, the phytoplankton population crashes (Keys, 2017). As the phytoplankton  
138 community was sampled over the transitional phase from diatoms and dinoflagellates to  
139 nanophytoplankton, the in situ silicate concentration was maintained to reproduce the silicate  
140 concentrations typical of this time of year (Smyth et al., 2010). Nutrient concentrations were  
141 measured at time point T0 only.

142 Media transfer and sample acquisition was driven by peristaltic pumps. Following 48 hrs  
143 acclimation in batch culture, semi-continuous daily dilution rates were maintained at between  
144 10-13 % of the incubation bottle volume throughout the experiment. CO<sub>2</sub> enriched seawater  
145 was added to the high CO<sub>2</sub> treatment replicates every 24 hrs, acclimating the natural  
146 phytoplankton population to increments of elevated pCO<sub>2</sub> from ambient to ~800 µatm over 8  
147 days followed by maintenance at ~800 µatm as per the method described by Schulz *et al*,  
148 (2009). Adding CO<sub>2</sub> enriched seawater is the preferred protocol, since some phytoplankton  
149 species are inhibited by the mechanical effects of direct bubbling (Riebesell et al., 2010; Shi et  
150 al., 2009) which causes a reduction in growth rates and the formation of aggregates (Love et al.,  
151 2016). pH was monitored daily to adjust the pCO<sub>2</sub> of the experimental media (+/-) prior to  
152 dilutions to maintain target pCO<sub>2</sub> levels in the incubation bottles. The seasonality in pH and total  
153 alkalinity (TA) are fairly stable at station L4 with high pH and low dissolved inorganic carbon  
154 (DIC) during early summer, and low pH, high DIC throughout autumn and winter (Kitidis et al.,  
155 2012). By maintaining the carbonate chemistry over the duration of the experiment, we aimed  
156 to simulate natural events at the study site.

157 To provide sufficient time for changes in the phytoplankton community to occur and to achieve  
158 an ecologically relevant data set, the incubation period was extended well beyond short-term  
159 acclimation. Previous pilot studies using the same experimental protocols highlighted that after  
160 ~20 days of incubation, significant changes in community structure and biomass were observed  
161 (Keys, 2017). These results were used to inform a more relevant incubation period of 30+ days.

## 162 **2.2 Analytical methods, experimental seawater**

### 163 **2.2.1 Chlorophyll *a***

164 Chl *a* was measured in each incubation bottle. 100 mL triplicate samples from each replicate  
165 were filtered onto 25 mm GF/F filters (nominal pore size 0.7 µm), extracted in 90 % acetone  
166 overnight at -20 °C and Chl *a* concentration was measured on a Turner Trilogy™ fluorometer  
167 using the non-acidified method of Welschmeyer (1994). The fluorometer was calibrated against

168 a stock Chl *a* standard (*Anacystis nidulans*, Sigma Aldrich, UK), the concentration of which was  
169 determined with a Perkin Elmer™ spectrophotometer at wavelengths 663.89 and 750.11 nm.  
170 Samples for Chl *a* analysis were taken every 2-3 days.

### 171 **2.2.2 Carbonate system**

172 70 mL samples for total alkalinity (TA) and dissolved inorganic carbon (DIC) analysis were  
173 collected from each experimental replicate, stored in amber borosilicate bottles with no head  
174 space and fixed with 40 µL of super-saturated Hg<sub>2</sub>Cl<sub>2</sub> solution for later determination (Apollo  
175 SciTech™ Alkalinity Titrator AS-ALK2; Apollo SciTech™ AS-C3 DIC analyser, with analytical  
176 precision of 3 µmol kg<sup>-1</sup>). Duplicate measurements were made for TA and triplicate  
177 measurements for DIC. Carbonate system parameter values for media and treatment samples  
178 were calculated from TA and DIC measurements using the programme CO<sub>2</sub>sys (Pierrot et al.,  
179 2006) with dissociation constants of carbonic acid of Mehrbach *et al.*, (1973) refitted by Dickson  
180 and Millero (Dickson and Millero, 1987). Samples for TA and DIC were taken for analysis every  
181 2-3 days throughout the experiment.

### 182 **2.2.3 Phytoplankton community analysis**

183 Phytoplankton community analysis was performed by flow cytometry (Becton Dickinson Accuri  
184 ™ C6) for the 0.2 to 18 µm size fraction following Tarran *et al.*, (2006) and inverted light  
185 microscopy was used to enumerate cells > 18 µm (BS EN 15204,2006). For flow cytometry, 2  
186 mL samples fixed with glutaraldehyde to a final concentration of 2 % were flash frozen in liquid  
187 nitrogen and stored at -80 °C for subsequent analysis. Phytoplankton data acquisition was  
188 triggered on both chlorophyll fluorescence and forward light scatter (FSC) using prior  
189 knowledge of the position of *Synechococcus* sp. to set the lower limit of analysis. Density plots of  
190 FSC vs. CHL fluorescence, phycoerythrin fluorescence vs. CHL fluorescence and side scatter  
191 (SSC) vs. CHL fluorescence were used to discriminate *Synechococcus* sp., picoeukaryote  
192 phytoplankton (approx. 0.5–3 µm), coccolithophores, cryptophytes, *Phaeocystis* sp. single cells  
193 and nanophytoplankton (eukaryotes >3 µm, excluding the coccolithophores, cryptophytes and  
194 *Phaeocystis* sp. single cells), (for further information on flow cytometer calibration for  
195 phytoplankton size measurements, see supplementary material). For inverted light microscopy,  
196 140 mL samples were fixed with 2 % (final concentration) acid Lugol's iodine solution and  
197 analysed by inverted light microscopy (Olympus™ IMT-2) using the Utermöhl counting  
198 technique (Utermöhl, 1958; Widdicombe *et al.*, 2010). Phytoplankton community samples were  
199 taken at T0, T10, T17, T24 and T36.

### 200 **2.2.4 Phytoplankton community biomass**

201 The smaller size fraction identified and enumerated through flow cytometry;  
202 picophytoplankton, nanophytoplankton, *Synechococcus*, coccolithophores and cryptophytes  
203 were converted to carbon biomass ( $\text{mg C m}^{-3}$ ) using a spherical model to calculate mean cell  
204 volume:

$$205 \left(\frac{4}{3} * \pi * r^3\right) \quad \text{Equation 1.}$$

206 and a conversion factor of  $0.22 \text{ pg C } \mu\text{m}^{-3}$  (Booth, 1988). A conversion factor of  $0.285 \text{ pg C } \mu\text{m}^{-3}$   
207 was used for coccolithophores (Tarran et al., 2006) and cell a volume of  $113 \mu\text{m}^3$  and carbon  
208 cell<sup>-1</sup> value of 18 pg applied for *Phaeocystis* spp. (Widdicombe et al., 2010). *Phaeocystis* spp.  
209 were identified and enumerated by flow cytometry separately to the nanophytoplankton class  
210 due to high observed abundance in in the high pCO<sub>2</sub> treatment. Mean cell measurements of  
211 individual species/taxa were used to calculate cell bio-volume for the  $18 \mu\text{m} +$  size fraction  
212 according to Kovalala and Larrance (1966) and converted to biomass according to the equations  
213 of Menden-Deuer & Lessard, (2000).

#### 214 **2.2.5 POC and PON**

215 Samples for particulate organic carbon (POC) and particulate organic nitrogen (PON) were  
216 taken at T0, T15 and T36.150 mL samples were taken from each replicate and filtered under  
217 gentle vacuum pressure onto pre-ashed 25mm glass fibre filters (GF/F, nominal pore size  $0.7$   
218  $\mu\text{m}$ ). Filters were stored in acid washed petri-slides at  $-20 \text{ }^\circ\text{C}$  until further processing. Sample  
219 analysis was conducted using a Thermoquest Elemental Analyser (Flash 1112). Acetanilide  
220 standards (Sigma Aldrich, UK) were used to calibrate measurements of carbon and nitrogen and  
221 also used during the analysis to account for possible drift in measured concentrations.

#### 222 **2.2.6 Chl fluorescence-based photophysiology**

223 Photosystem II (PSII) variable chlorophyll fluorescence parameters were measured using a fast  
224 repetition rate fluorometer (FRRf) (FastOcean sensor in combination with an Act2Run  
225 laboratory system, Chelsea Technologies, West Molesey, UK). The excitation wavelengths of the  
226 FRRf's light emitting diodes (LEDs) were 450, 530 and 624 nm. The instrument was used in  
227 single turnover mode with a saturation phase comprising 100 flashlets on a  $2 \mu\text{s}$  pitch and a  
228 relaxation phase comprising 40 flashlets on a  $50 \mu\text{s}$  pitch. Measurements were conducted in a  
229 temperature-controlled chamber at  $15 \text{ }^\circ\text{C}$ . The minimum ( $F_o$ ) and maximum ( $F_m$ ) Chl  
230 fluorescence were estimated according to Kolber et al., (1998). Maximum quantum yields of PSII  
231 were calculated as:

$$232 F_v / F_m = (F_m - F_o) / F_m \quad \text{Equation 2.}$$

233 PSII electron flux was calculated on a volume basis ( $JV_{PSII}$ ;  $\text{mol e}^- \text{m}^{-3} \text{d}^{-1}$ ) using the absorption  
234 algorithm (Oxborough et al., 2012) following spectral correction by normalising the FRRf LED  
235 emission to the white spectra using Fast<sup>PRO</sup> 8 software. This step required inputting the  
236 experimental phytoplankton community fluorescence excitation spectra values (FES). Since we  
237 did not measure the FES of our experimental samples, we used mean literature values for each  
238 phytoplankton group calculated proportionally (based on percentage contribution to total  
239 estimated biomass per phytoplankton group) as representative values for our experimental  
240 samples. The  $JV_{PSII}$  rates were converted to chlorophyll specific carbon fixation rates ( $\text{mg C (mg}$   
241  $\text{Chl } a)^{-1} \text{m}^{-3} \text{h}^{-1}$ ), calculated as:

$$242 \quad JV_{PSII} \times \varphi_{E:C} \times MW_C / \text{Chl } a \quad \text{Equation 3}$$

243 where  $\varphi_{E:C}$  is the electron requirement for carbon uptake ( $\text{molecule CO}_2 \text{ (mol electrons)}^{-1}$ ),  $MW_C$   
244 is the molecular weight of carbon and  $\text{Chl } a$  is the  $\text{Chl } a$  measurement specific to each sample.  
245  $\text{Chl } a$  specific  $JV_{PSII}$  based photosynthesis-irradiance curves were conducted in replicate batches  
246 between 10:00 – 16:00 to account for variability over the photo-period at between 8 - 14  
247 irradiance intensities. The maximum intensity applied was adjusted according to ambient  
248 natural irradiance on the day of sampling. Maximum photosynthetic rates of carbon fixation  
249 ( $P^B_m$ ), the light limited slope ( $\alpha^B$ ) and the light saturation point of photosynthesis ( $I_k$ ) were  
250 estimated by fitting the data to the model of Webb et al., (1974):

$$251 \quad P^B = (1 - e^{-\alpha \times I / P^B_m}) \quad \text{Equation 4}$$

252 Due to instrument failure during the experiment, samples for FRRf fluorescence-based light  
253 curves were taken at T36 only.

### 254 **2.3 Statistical analysis**

255 To test for effects of temperature,  $p\text{CO}_2$  and possible time dependence of the measured response  
256 variables ( $\text{Chl } a$ , total biomass, POC, PON, photosynthetic parameters and biomass of individual  
257 species), generalized linear mixed models with the factors  $p\text{CO}_2$ , temperature and time (and all  
258 interactions) were applied to the data between T0 and T36. Analyses were conducted using the  
259 lme4 package in R (R Core Team (2014). R Foundation for Statistical Computing, Vienna,  
260 Austria).

## 261 **3. Results**

262  $\text{Chl } a$  concentration in the WEC at station L4 from 30 September - 6<sup>th</sup> October 2015 (when sea  
263 water was collected for the experiment) varied between 0.02-5  $\text{mg m}^{-3}$ , with a mean  
264 concentration of  $\sim 1.6 \text{ mg m}^{-3}$  (**Fig. 1 A**). Over the period leading up to phytoplankton  
265 community sampling, increasing nitrate and silicate concentrations coincided with a  $\text{Chl } a$  peak



266 on 23<sup>rd</sup> September (**Fig. 1 B**). Routine net trawl (20  $\mu\text{m}$ ) sample observations indicated a  
267 phytoplankton community dominated by the diatoms *Leptocylindrus danicus* and *L. minimus*  
268 with a lower presence of the dinoflagellates *Prorocentrum cordatum*, *Heterocapsa* spp. and  
269 *Oxytoxum gracile*. Following decreasing nitrate concentrations, there was a *P. cordatum* bloom  
270 on 29<sup>th</sup> September, during the week before the experiment started (data not shown).

### 271 **3.1 Experimental carbonate system**

272 Equilibration to the target high  $\text{pCO}_2$  values (800  $\mu\text{atm}$ ) within the high  $\text{pCO}_2$  and combination  
273 treatments was achieved at T10 (**Fig. 2 A & B**). These treatments were slowly acclimated to  
274 increasing levels of  $\text{pCO}_2$  over 7 days (from the initial dilution at T3) while the control and high  
275 temperature treatments were acclimated at the same ambient carbonate system values as those  
276 measured at station L4 on the day of sampling. Following equilibration, the mean  $\text{pCO}_2$  values  
277 within the control and high temperature treatments were 394.9 ( $\pm 4.3$  sd) and 393.2 ( $\pm 4.8$  sd)  
278  $\mu\text{atm}$  respectively, while in the high  $\text{pCO}_2$  and combination treatments mean  $\text{pCO}_2$  values were  
279 822.6 ( $\pm 9.4$ ) and 836.5 ( $\pm 15.6$  sd)  $\mu\text{atm}$ , respectively. Carbonate system values remained stable  
280 throughout the experiment (For full carbonate system measured and calculated parameters, see  
281 **Table S1** in supplementary material).

### 282 **3.2 Experimental temperature treatments**

283 Mean temperatures in the control and high  $\text{pCO}_2$  treatments were 14.1 ( $\pm 0.35$  sd)  $^\circ\text{C}$  and in the  
284 high temperature and combination treatments the mean temperatures were 18.6 ( $\pm 0.42$  sd)  $^\circ\text{C}$ ,  
285 with a mean temperature difference between the ambient and high temperature treatments of  
286 4.46 ( $\pm 0.42$  sd)  $^\circ\text{C}$  (Supplementary material, **Fig. S2 A & B**).

287

### 288 **3.3 Chlorophyll *a***

289 Mean Chl *a* in the experimental seawater at T0 was 1.64 ( $\pm 0.02$  sd)  $\text{mg m}^{-3}$  (**Fig. 3 A**). This  
290 decreased in all treatments between T0 to T7, to  $\sim 0.1$  ( $\pm 0.09$ , 0.035 and 0.035 sd)  $\text{mg m}^{-3}$  in the  
291 control, high  $\text{pCO}_2$  and combination treatments, while in the high temperature treatment at T7  
292 Chl *a* was 0.46  $\text{mg m}^{-3}$  ( $\pm 0.29$  sd) ( $z = 2.176$ ,  $p < 0.05$ ). From T7 to T12 Chl *a* increased in all  
293 treatments which was highest in the combination (4.99  $\text{mg m}^{-3} \pm 0.69$  sd) and high  $\text{pCO}_2$   
294 treatments (3.83  $\text{mg m}^{-3} \pm 0.43$  sd). Overall, Chl *a* was significantly influenced by experimental  
295 time, independent of experimental treatments (**Table 1**). At T36 Chl *a* concentration in the  
296 combination treatment was higher (6.87 ( $\pm 0.58$  sd)  $\text{mg m}^{-3}$ ) than all other treatments while the  
297 high temperature treatment concentration was higher (4.77 ( $\pm 0.44$  sd)  $\text{mg m}^{-3}$ ) than the control  
298 and high  $\text{pCO}_2$  treatment. Mean concentrations for the control and high  $\text{pCO}_2$  treatment at T36

299 were not significantly different at  $3.30 (\pm 0.22 \text{ sd})$  and  $3.46 (\pm 0.35 \text{ sd}) \text{ mg m}^{-3}$  respectively  
300 (pairwise comparison  $t = 0.78, p = 0.858$ ).

### 301 **3.4 Phytoplankton biomass**

302 The starting biomass in all treatments was  $110.2 (\pm 5.7 \text{ sd}) \text{ mg C m}^{-3}$  (**Fig. 3 B**). The biomass was  
303 dominated by dinoflagellates ( $\sim 50\%$ ) with smaller contributions from nanophytoplankton  
304 ( $\sim 13\%$ ), cryptophytes ( $\sim 11\%$ ), diatoms ( $\sim 9\%$ ), coccolithophores ( $\sim 8\%$ ), *Synechococcus* ( $\sim 6\%$ )  
305 and picophytoplankton ( $\sim 3\%$ ). Total biomass was significantly influenced in all treatments over  
306 time (**Table 1**) and at T10, it was significantly higher in the high temperature treatment when  
307 biomass reached  $752 (\pm 106 \text{ sd}) \text{ mg C m}^{-3}$  ( $z = 2.769, p < 0.01$ ). Biomass was significantly higher  
308 in the elevated pCO<sub>2</sub> treatment (interaction of time x high pCO<sub>2</sub>) (**Table 1**), reaching  $2481 (\pm$   
309  $182.68 \text{ sd}) \text{ mg C m}^{-3}$  at T36,  $\sim 6.5$ -fold higher than the control ( $z = 3.657, p < 0.001$ ). Total  
310 biomass in the high temperature treatment at T36 was significantly higher than the  
311 combination treatment and ambient control ( $z = 2.744, p < 0.001$ ), which were  $525 (\pm 28.02 \text{ sd})$   
312  $\text{mg C m}^{-3}$  and  $378 (\pm 33.95 \text{ sd}) \text{ mg C m}^{-3}$ , respectively. Reaching  $1735 (\pm 169.24 \text{ sd}) \text{ mg C m}^{-3}$ ,  
313 biomass in the high temperature treatment was  $\sim 4.6$ -fold higher than the control.

314 POC followed the same trends in all treatments between T0 and T36 (**Fig. 3 C**) and was in close  
315 range of the estimated biomass ( $R^2 = 0.914$ , **Fig. 3 D**). POC was significantly influenced by the  
316 interaction of time x high pCO<sub>2</sub> and time x high temperature (**Table 1**). At T36 POC was  
317 significantly higher in the high pCO<sub>2</sub> treatment ( $2086 \pm 155.19 \text{ sd mg m}^{-3}$ ) followed by the high  
318 temperature treatment ( $1594 \pm 162.24 \text{ sd mg m}^{-3}$ ),  $\sim 5.4$ -fold and 4-fold higher than the control,  
319 respectively. whereas a decline in POC was observed in the control and combination treatment.  
320 PON followed the same trend as POC over the course of the experiment, though it was only  
321 significantly influenced by the interaction between time x high pCO<sub>2</sub> (**Fig. 3 E, Table 1**). At T36  
322 concentrations were  $147 (\pm 12.99 \text{ sd})$  and  $133 (\pm 15.59 \text{ sd}) \text{ mg m}^{-3}$  in the high pCO<sub>2</sub> and high  
323 temperature treatments respectively, while PON was  $57.75 (\pm 13.07 \text{ sd}) \text{ mg m}^{-3}$  in the  
324 combination treatment and  $47.18 (\pm 9.32 \text{ sd}) \text{ mg m}^{-3}$  in the control. POC:PON ratios were  
325 significantly influenced by the interaction of time x high pCO<sub>2</sub> and time x high temperature  
326 (**Table 1**). The largest increase, from  $3.028 \times 10^{-5}$  to  $1.632 \times 10^{-4} \mu\text{M C}:\mu\text{M N}$  ( $\pm 1.299 \times 10^{-5} \text{ sd}$ )  
327 was in the high pCO<sub>2</sub> treatment (4.5-fold higher than the control at T36), followed by an  
328 increase to  $1.232 \times 10^{-4} (\pm 1.404 \times 10^{-5} \text{ sd}) \mu\text{M C}:\mu\text{M N}$  in the high temperature treatment (3-  
329 fold higher than the control at T36). POC:PON in the combination treatment also increased over  
330 time and was 45% higher than the control at T36 ( $4.200 \times 10^{-5} \pm 5.550 \times 10^{-6} \text{ sd}) \mu\text{M C}:\mu\text{M N}$   
331 (**Fig. 3 F**).

### 332 **3.5 Community composition**

333 From T0 to T24 the community shifted away from dominance of dinoflagellates in all  
334 treatments, followed by further regime shifts between T24 and T36 in the control and  
335 combination treatments. At T36 diatoms dominated the phytoplankton community biomass in  
336 the ambient control (**Fig. 4 A**), while the high temperature and high pCO<sub>2</sub> treatments exhibited  
337 near mono-specific dominance of nanophytoplankton (**Figs. 4 B & C**). The most diverse  
338 community was in the combination treatment where dinoflagellates and *Synechococcus* became  
339 more prominent (**Fig. 4 D**).

340 Between T10 and T24 the community shifted to nanophytoplankton in all experimental  
341 treatments. This dominance was maintained to T36 in the high temperature and high pCO<sub>2</sub>  
342 treatments whereas in the ambient control and combination treatment, the community shifted  
343 away from nanophytoplankton (**Fig. 5 A**). Nanophytoplankton biomass was significantly higher  
344 in the high pCO<sub>2</sub> treatment (**Table 2**) with biomass reaching 2216 ( $\pm 189.67$  sd) mg C m<sup>-3</sup> at  
345 T36. This biomass was also high (though not significantly throughout the experiment until T36)  
346 in the high temperature treatment (T36: 1489 ( $\pm 170.32$  sd) mg C m<sup>-3</sup>,  $z = 1.695$ ,  $p = 0.09$ )  
347 compared to the control and combination treatments. In the combination treatment  
348 nanophytoplankton biomass was 238 ( $\pm 14.16$  sd) mg C m<sup>-3</sup> at T36 which was higher than the  
349 control, though not significantly ( $162 \pm 20.02$  sd mg C m<sup>-3</sup>). In addition to significant differences  
350 in nanophytoplankton biomass amongst the experimental treatments, treatment-specific  
351 differences in cell size were also observed. Larger nano-flagellates dominated the control (mean  
352 cell diameter of 6.34  $\mu$ m), smaller nano-flagellates dominated the high temperature and  
353 combination treatments (mean cell diameters of 3.61  $\mu$ m and 4.28  $\mu$ m) whereas *Phaeocystis* spp.  
354 dominated the high pCO<sub>2</sub> treatment (mean cell diameter 5.04  $\mu$ m) and was not observed in any  
355 other treatment (Supplementary material, **Fig. S3 A-D**).

356 At T0, diatom biomass was low and dominated by *Coscinodiscus wailessi* (48 %; 4.99 mg C m<sup>-3</sup>),  
357 *Pleurosigma* (25 %; 2.56 mg C m<sup>-3</sup>) and *Thalassiosira subtilis* (19 %; 1.94 mg C m<sup>-3</sup>). Small  
358 biomass contributions were made by *Navicula distans*, undetermined pennate diatoms and  
359 *Cylindrotheca closterium*. Biomass in the diatom group remained low from T0 to T24 but  
360 increased significantly through time in all treatments (**Table 2**), with the highest biomass in the  
361 high pCO<sub>2</sub> treatment ( $235 \pm 21.41$  sd mg C m<sup>-3</sup>, **Fig. 5 B**). The highest diatom contribution to  
362 total community biomass at T36 was in the ambient control (52 % of biomass;  $198 \pm 17.28$  sd  
363 mg C m<sup>-3</sup>). In both the high temperature and combination treatments diatom biomass was lower  
364 at T36 ( $151 \pm 10.94$  sd and  $124 \pm 19.16$  sd mg C m<sup>-3</sup>, respectively). In all treatments, diatom  
365 biomass shifted from the larger *C. wailessi* to the smaller *C. closterium*, *N. distans*, *T. subtilis* and  
366 *Tropidoneis* spp., the relative contributions of which were treatment-specific. Overall *N. distans*  
367 dominated diatom biomass in all treatments at T36 (ambient control:  $112 \pm 24.86$  sd mg C m<sup>-3</sup>,

368 56 % of biomass; high temperature:  $106 \pm 17.75$  sd mg C m<sup>-3</sup>, 70 % of biomass; high pCO<sub>2</sub>:  $152 \pm$   
369  $19.09$  sd mg C m<sup>-3</sup>, 61 % of biomass; and combination:  $111 \pm 20.97$  sd mg C m<sup>-3</sup>, 89 % of  
370 biomass; Supplementary material, **Fig. S4 A-D**).

371 The starting dinoflagellate community was dominated by *Gyrodinium spirale* (91 %; 49 mg C m<sup>-3</sup>),  
372 with smaller contributions from *Katodinium glaucum* (5 %; 2.76 mg C m<sup>-3</sup>), *Prorocentrum*  
373 *cordatum* (3 %; 1.78 mg C m<sup>-3</sup>) and undetermined *Gymnodiniales* (1 %; 0.49 mg C m<sup>-3</sup>). At T36  
374 Dinoflagellate biomass was significantly higher in the combination treatment ( $90 \pm 16.98$  sd mg  
375 C m<sup>-3</sup>, **Fig. 5 C, Table 2**) followed by the high temperature treatment ( $57 \pm 6.87$  sd mg C m<sup>-3</sup>,  
376 **Table 2**). There was no significant difference in dinoflagellate biomass between the high pCO<sub>2</sub>  
377 treatment and ambient control at T36 when biomass was low. In the combination treatment, the  
378 dinoflagellate biomass became dominated by *P. cordatum* which contributed  $59 \pm 12.95$  sd mg C  
379 m<sup>-3</sup> (66 % of biomass in this group).

380 *Synechococcus* biomass was significantly higher in the combination treatment (reaching  $59.9 \pm$   
381  $4.30$  sd mg C m<sup>-3</sup> at T36, **Fig. 5 D, Table 2**) followed by the high temperature treatment ( $30 \pm$   
382  $5.98$  sd mg C m<sup>-3</sup>, **Table 2**). In both the high pCO<sub>2</sub> treatment and control *Synechococcus* biomass  
383 was low ( $\sim 7$  mg C m<sup>-3</sup> in both treatments at T36), though an initial significant response to high  
384 pCO<sub>2</sub> was observed between T0 – T10 (**Table 2**). In all treatments and throughout the  
385 experiment, relative to the other phytoplankton groups, biomass of picophytoplankton (**Fig. 5**  
386 **E**), cryptophytes (**Fig. 5 F**) and coccolithophores (**Fig. 5 G**) remained low, though there was a  
387 slight increase in picophytoplankton in the combination treatment ( $11.26 \pm 0.79$  sd mg C m<sup>-3</sup>;  
388 **Table 2**).

389 Microzooplankton was dominated by *Strombolidium* spp. in all treatments throughout the  
390 experiment, though biomass was low relative to the phytoplankton community (**Fig. 6**).  
391 Following a decline from T0 to T10, microzooplankton biomass increased in all but the high CO<sub>2</sub>  
392 treatment until T17 when biomass diverged. The biomass trajectory maintained an increase in  
393 the control when at T36 it was highest at  $\sim 1.6$  mg C m<sup>-3</sup>, 90% higher than the high temperature  
394 treatment ( $0.83$  mg C m<sup>-3</sup>). Microzooplankton biomass was significantly lower in the high CO<sub>2</sub>  
395 treatment at T36 ( $z = -2.100$ ,  $p = 0.036$ ) and undetected in the combination treatment at this  
396 time point (**Table 2**).

397

### 398 **3.6 Chl *a* fluorescence-based photophysiology**

399 At T36, FRRf photosynthesis-irradiance (PE) parameters were strongly influenced by the  
400 experimental treatments. P<sup>B<sub>m</sub></sup> was significantly higher in the high pCO<sub>2</sub> treatment ( $18.93$  mg C

401 (mg Chl *a*)<sup>-1</sup> m<sup>-3</sup> h<sup>-1</sup>), followed by the high temperature treatment (9.58 mg C (mg Chl *a*)<sup>-1</sup> m<sup>-3</sup> h<sup>-1</sup>;  
402 **Fig. 7, Tables 3 & 4**). There was no significant difference in P<sup>B<sub>m</sub></sup> between the control and  
403 combination treatments (2.77 and 3.02 mg C (mg Chl *a*)<sup>-1</sup> m<sup>-3</sup> h<sup>-1</sup>). Light limited photosynthetic  
404 efficiency (α<sup>B</sup>) also followed the same trend and was significantly higher in the high pCO<sub>2</sub>  
405 treatment (0.13 mg C (mg Chl *a*)<sup>-1</sup> m<sup>-3</sup> h<sup>-1</sup> (μmol photon m<sup>-2</sup> s<sup>-1</sup>)<sup>-1</sup>) followed by the high  
406 temperature treatment (0.09 mg C (mg Chl *a*)<sup>-1</sup> m<sup>-3</sup> h<sup>-1</sup> (μmol photon m<sup>-2</sup> s<sup>-1</sup>)<sup>-1</sup>; **Tables 3 & 4**). α<sup>B</sup>  
407 was low in both the control and combination treatment (0.03 and 0.04 mg C (mg Chl *a*)<sup>-1</sup> m<sup>-3</sup> h<sup>-1</sup>  
408 (μmol photon m<sup>-2</sup> s<sup>-1</sup>)<sup>-1</sup>, respectively). The light saturation point of photosynthesis (*E<sub>k</sub>*) was  
409 significantly higher in the high pCO<sub>2</sub> treatment relative to all treatments (144.13 μmol photon  
410 m<sup>-2</sup> s<sup>-1</sup>), though significantly lower in the combination treatment relative to both the high pCO<sub>2</sub>  
411 and high temperature treatments (**Tables 3 & 4**).

#### 412 **4. Discussion**

413 Individually, elevated temperature and pCO<sub>2</sub> resulted in the highest biomass and maximum  
414 photosynthetic rates (P<sup>B<sub>m</sub></sup>) at T36, when nanophytoplankton dominated. The interaction of  
415 these two factors had little effect on total biomass with values close to the ambient control, and  
416 no effect on P<sup>B<sub>m</sub></sup>. The combination treatment, however, exhibited the greatest diversity of  
417 phytoplankton functional groups with dinoflagellates and *Synechococcus* becoming dominant  
418 over time.

419 Elevated pCO<sub>2</sub> has been shown to enhance the growth and photosynthesis of some  
420 phytoplankton species which have active uptake systems for inorganic carbon (Giordano et al.,  
421 2005; Reinfelder, 2011). Elevated pCO<sub>2</sub> may therefore lead to lowered energetic costs of carbon  
422 assimilation in some species and a redistribution of the cellular energy budget to other  
423 processes (Tortell et al., 2002). In this study, under elevated pCO<sub>2</sub> where the dominant group  
424 was nanophytoplankton, the most abundant species was the haptophyte *Phaeocystis* spp.  
425 Photosynthetic carbon fixation in *Phaeocystis* spp. is presently near saturation with respect to  
426 current levels of pCO<sub>2</sub> (Rost et al., 2003). Dominance of this spp. under elevated pCO<sub>2</sub> may be  
427 due to lowered grazing pressure since microzooplankton biomass was lowest in the high CO<sub>2</sub>  
428 treatment throughout the experiment. The increased biomass and photosynthetic carbon  
429 fixation in this experimental community under elevated pCO<sub>2</sub> is due to the community shift to  
430 *Phaeocystis* spp.. The increased biomass in the high temperature treatment (where  
431 microzooplankton biomass remained stable between T17 to T36, though lower than the  
432 control) may be attributed to enhanced enzymatic activities, since algal growth commonly  
433 increases with temperature until after an optimal range (Boyd et al., 2013; Goldman and  
434 Carpenter, 1974; Savage et al., 2004). Optimum growth temperatures for marine phytoplankton  
435 are often several degrees higher than environmental temperatures (Eppley, 1972; Thomas et al.,

436 2012). Nanophytoplankton also dominated in this treatment and while *Phaeocystis* spp. was not  
437 discriminated, no further classification was made at a group/species level. Reduced biomass in  
438 the control from T24 onwards may be due to increased grazing pressure given the highest  
439 concentrations of microzooplankton biomass were observed in the control. Conversely,  
440 microzooplankton biomass declined significantly from T17 in the combination treatment,  
441 indicating reduced grazing pressure while phytoplankton biomass also declined from this time  
442 point. Nutrient concentrations were not measured beyond T0 and we cannot therefore exclude  
443 the possibility that differences in nutrient availability may have contributed to observed  
444 differences between control and high temperature and high CO<sub>2</sub> treatments.

#### 445 **4.1 Chl *a***

446 Biomass in the control peaked at T25 followed by a decline to T36. Correlated with this, Chl *a*  
447 also peaked at T25 in the control and declined to 3.3 mg m<sup>-3</sup> by T27, remaining close to this  
448 value until T36. Biomass in the combination treatment peaked at T20 followed by decline to  
449 T36 whereas Chl *a* in this treatment declined from T20 to T25 followed by an increase at T27  
450 before further decline similar to the biomass. Chl *a* peaked in this treatment again at T36 (6.8  
451 mg m<sup>-3</sup>). We attribute the increase in Chl *a* between T25 – T27 (coincident with an overall  
452 biomass decrease) to lower species specific carbon:Chl *a* ratios as a result of the increase in  
453 dinoflagellates, *Synechococcus* and picophytoplankton biomass from T25. We speculate that the  
454 decline in biomass under nutrient replete conditions in the combination treatment was  
455 probably due to slower species-specific growth rates when diatoms and dinoflagellates became  
456 more prominent in this treatment. Carbon:Chl *a* in diatoms and dinoflagellates have previously  
457 been demonstrated to be lower than nano- and picophytoplankton (Sathyendranath et al.,  
458 2009) This contrasts the results reported in comparable studies as Chl *a* is generally highly  
459 correlated with biomass, ( e.g. Feng et al., 2009). Similar results were reported however by Hare  
460 et al., (2007) which indicates that Chl *a* may not always be a reliable proxy for biomass in mixed  
461 communities.

#### 462 **4.2 Biomass**

463 This study shows that the phytoplankton community response to elevated temperature and  
464 pCO<sub>2</sub> is highly variable. pCO<sub>2</sub> elevated to ~800 μatm induced higher community biomass, similar  
465 to the findings of Kim et al., (2006), whereas in other natural community studies no CO<sub>2</sub> effect  
466 on biomass was observed (Delille et al., 2005; Maudengre et al., 2017; Paul et al., 2015). A ~4.5  
467 °C increase in temperature also resulted in higher biomass at T36 in this study, similar to the  
468 findings of Feng et al., (2009) and Hare et al., (2007) though elevated temperature has  
469 previously reduced biomass of natural nanophytoplankton communities in the Western Baltic

470 Sea and Arctic Ocean (Coello-Camba et al., 2014; Moustaka-Gouni et al., 2016). When elevated  
471 temperature and pCO<sub>2</sub> were combined, community biomass exhibited little response, similar to  
472 the findings of Gao et al., (2017), though an increase in biomass has also been reported (Calbet  
473 et al., 2014; Feng et al., 2009). Geographic location and season also play an important role in  
474 structuring the community and its response in terms of biomass to elevated temperature and  
475 pCO<sub>2</sub>. (Li et al., 2009; Morán et al., 2010). This may explain part of the variability in responses  
476 observed from studies on phytoplankton during different seasons and provinces.

#### 477 **4.3 Carbon:Nitrogen**

478 In agreement with others, the results of this experiment showed highest increases in C:N under  
479 elevated pCO<sub>2</sub> alone (Riebesell et al., 2007). C:N also increased under high temperature,  
480 consistent with the findings of Lomas and Glibert, (1999) and Taucher et al., (2015). It also  
481 increased when pCO<sub>2</sub> and temperature were elevated, albeit to a lesser degree, which was also  
482 observed by Calbet et al., (2014), but contrasts other studies that have observed C:N being  
483 unaffected by the combined influence of elevated pCO<sub>2</sub> and temperature (Deppeler and  
484 Davidson, 2017; Kim et al., 2006; C. Paul et al., 2015). C:N is a strong indicator of cellular protein  
485 content (Woods and Harrison, 2003) and increases under elevated pCO<sub>2</sub> and warming may lead  
486 to lowered nutritional value of phytoplankton which has implications for zooplankton  
487 reproduction and the biogeochemical cycling of nutrients.

#### 488 **4.4 Photosynthetic carbon fixation rates**

489 At T36, under elevated pCO<sub>2</sub> P<sup>B</sup><sub>m</sub> was > 6 times higher than in the control, but only one time  
490 point was measured so we are not able to make decisive conclusions. Riebesell et al., (2007) and  
491 Tortell et al., (2008) also reported an increase in P<sup>B</sup><sub>m</sub> under elevated pCO<sub>2</sub>. By contrast other  
492 observations on natural populations under elevated pCO<sub>2</sub> reported a reduction in P<sup>B</sup><sub>m</sub> (Feng et  
493 al., 2009; Hare et al., 2007). Studies on laboratory cultures have shown that increases in  
494 temperature cause an increase photosynthetic rates (Feng et al., 2008; Fu et al., 2007; Hutchins  
495 et al., 2007), similar to what we observed in this study. In the combined pCO<sub>2</sub> and temperature  
496 treatment, we found no effect on P<sup>B</sup><sub>m</sub>, which has also been observed in experiments on natural  
497 populations (Coello-Camba and Agustí, 2016; Gao et al., 2017). This contrasts the findings of  
498 Feng et al., (2009) and Hare et al., (2007) who observed the highest P<sup>B</sup><sub>m</sub> when temperature and  
499 pCO<sub>2</sub> were elevated simultaneously. In this study, increases in  $\alpha^B$  and  $E_k$  under elevated pCO<sub>2</sub>,  
500 and a decrease in these parameters when elevated pCO<sub>2</sub> and temperature were combined also  
501 contrasts the trends reported by Feng et al., (2009). We should stress however, that while our  
502 photophysiological measurements support our observed trends in community biomass, they

503 were made on a single occasion at the end of the experiment. Future experiments should focus  
504 on acquiring photophysiological measurements throughout.

505 Species specific photosynthetic rates have been demonstrated to decrease beyond their thermal  
506 optimum (Raven and Geider, 1988) which can be modified through photoprotective rather than  
507 photosynthetic pigments (Kiefer and Mitchell, 1983). This may explain the difference in  $P^B_m$   
508 between the high  $pCO_2$  and high temperature treatments (in addition to differences in  
509 nanophytoplankton community composition in relation to *Phaeocystis* spp. discussed above), as  
510 the experimental high temperature treatment in this study was  $\sim 4.5$  ° C higher than the control.

511 There was no significant effect of combined elevated  $pCO_2$  and temperature on  $P^B_m$ , which was  
512 strongly influenced by taxonomic differences between the experimental treatments. Warming  
513 has been shown to lead to smaller cell sizes in nanophytoplankton (Atkinson et al., 2003; Peter  
514 and Sommer, 2012), which was observed in the combined treatment together with decreased  
515 nanophytoplankton biomass. Diatoms also shifted to smaller species with reduced biomass,  
516 while dinoflagellate and *Synechococcus* biomass increased at T36. Dinoflagellates are the only  
517 photoautotrophs with form II RuBisCO (Morse et al., 1995) which has the lowest  
518 carboxylation:oxygenation specificity factor among eukaryotic phytoplankton (Badger et al.,  
519 1998), which may give dinoflagellates a disadvantage in carbon fixation under present ambient  
520  $pCO_2$  levels. Phytoplankton growth rates are generally slower in surface waters with high pH  
521 ( $\geq 9$ ) resulting from photosynthetic removal of  $CO_2$  by previous blooms and the associated  
522 nutrient depletion (Hansen, 2002; Hinga, 2002). Though growth under high pH provides  
523 indirect evidence that dinoflagellates possess CCMs, direct evidence is limited and points to the  
524 efficiency of CCMs in dinoflagellates as moderate in comparison to diatoms and some  
525 haptophytes (Reinfelder, 2011 and references therein). Given that dinoflagellates accounted for  
526 just  $\sim 20\%$  of biomass in the combination treatment, exerting a minor influence on community  
527 photosynthetic rates, further work is required to explain the lower  $P^B_m$  under the combined  
528 influence of elevated  $pCO_2$  and temperature compared to the individual treatment influences.  
529 We applied the same electron requirement parameter for carbon uptake across all treatments,  
530 though in nature and between species, there can be considerable variation in this parameter  
531 (e.g. 1.15 to 54.2 mol  $e^-$  (mol C) $^{-1}$ ; Lawrenz et al., 2013) which can co-vary with temperature,  
532 nutrients, Chl *a*, irradiance and community structure. Better measurement techniques at  
533 quantifying this variability are necessary in the future.

#### 534 **4.5 Community composition**

535 Phytoplankton community structure changes were observed, with a shift from dinoflagellates to  
536 nanophytoplankton which was most pronounced under single treatments of elevated



537 temperature and pCO<sub>2</sub>. Amongst the nanophytoplankton, a distinct size shift to smaller cells was  
538 observed in the high temperature and combination treatments, while in the high pCO<sub>2</sub>  
539 treatment *Phaeocystis* spp. dominated. Under combined pCO<sub>2</sub> and temperature from T24  
540 onwards however, dinoflagellate and *Synechococcus* biomass increased and nanophytoplankton  
541 biomass decreased. An increase in pico- and nanophytoplankton has previously been reported  
542 in natural communities under elevated pCO<sub>2</sub> (Bermúdez et al., 2016; Boras et al., 2016;  
543 Brussaard et al., 2013; Engel et al., 2008) while no effect on these size classes has been observed  
544 in other studies (Calbet et al., 2014; Paulino et al., 2007). Moustaka-Gouni et al., (2016) also  
545 found no CO<sub>2</sub> effect on natural nanophytoplankton communities but increased temperature  
546 reduced the biomass of this group. Kim et al., (2006) observed a shift from nanophytoplankton  
547 to diatoms under elevated pCO<sub>2</sub> alone while a shift from diatoms to nanophytoplankton under  
548 combined elevated pCO<sub>2</sub> and temperature has been reported (Hare et al., 2007). A variable  
549 response in *Phaeocystis* spp. to elevated pCO<sub>2</sub> has also been reported with increased growth  
550 (Chen et al., 2014; Keys et al., 2017), no effect (Thoisen et al., 2015) and decreased growth  
551 (Hoogstraten et al., 2012) observed. *Phaeocystis* spp. can outcompete other phytoplankton and  
552 form massive blooms (up to 10 g C m<sup>-3</sup>) with impacts on food webs, global biogeochemical  
553 cycles and climate regulation (Schoemann et al., 2005). While not a toxic algal species,  
554 *Phaeocystis* spp. are considered a harmful algal bloom (HAB) species when biomass reaches  
555 sufficient concentrations to cause anoxia through the production of mucus foam which can clog  
556 the feeding apparatus of zooplankton and fish (Eilertsen & Raa, 1995).

557 Recently published studies on the response of diatoms to elevated pCO<sub>2</sub> and temperature vary  
558 greatly. For example, Taucher et al., (2015) showed that *Thalassiosira weissflogii* incubated at  
559 1000 µatm pCO<sub>2</sub> increased growth by 8 % while for *Dactyliosolen fragilissimus*, growth  
560 increased by 39 %; temperature elevated by + 5°C also had a stimulating effect on *T. weissflogii*  
561 but inhibited the growth rate of *D. fragilissimus*; and when the treatments were combined  
562 growth was enhanced in *T. weissflogii* but reduced in *D. fragilissimus*. In our study, elevated pCO<sub>2</sub>  
563 increased biomass in diatoms (time dependent), but elevated temperature and the combination  
564 of these factors reduced the signal of this response. A distinct size-shift in diatom species was  
565 observed in all treatments, from the larger *Coscinodiscus* spp., *Pleurosigma* and *Thalassiosira*  
566 *subtilis* to the smaller *Navicula distans*. This was most pronounced in the combination treatment  
567 where *N. distans* formed 89 % of diatom biomass. *Navicula* spp. previously exhibited a  
568 differential response to both elevated temperature and pCO<sub>2</sub>. At + 4.5 °C and 960 ppm CO<sub>2</sub>  
569 Torstensson et al., (2012) observed no synergistic effects on the benthic *Navicula directa*.  
570 Elevated temperature increased growth rates by 43 % while a reduction of 5 % was observed  
571 under elevated CO<sub>2</sub>. No effects on growth were detected at pH ranging from 8 – 7.4 units in

572 *Navicula* spp. (Thoisen et al., 2015), while there was a significant increase in growth in *N.*  
573 *distans* along a CO<sub>2</sub> gradient at a shallow cold-water vent system (Baragi et al., 2015).

574 *Synechococcus* grown under pCO<sub>2</sub> elevated to 750 ppm and temperature elevated by 4 °C  
575 resulted in increased growth and a 4-fold increase in P<sup>B</sup><sub>m</sub> (Fu et al., 2007) which is similar to the  
576 results of the present study.

577 The combination of elevated temperature and pCO<sub>2</sub> significantly increased dinoflagellate  
578 biomass to 17 % of total biomass. This was due to *P. cordatum* which increased biomass by  
579 more than 30-fold from T0 to T30 (66 % of dinoflagellate biomass in this treatment). Despite  
580 the global increase in the frequency of HABs few studies have focussed on the response of  
581 dinoflagellates to elevated pCO<sub>2</sub> and temperature. In laboratory studies at 1000 ppm CO<sub>2</sub>,  
582 growth rates of the HAB species *Karenia brevis* increased by 46 %, at 1000 ppm CO<sub>2</sub> and + 5 °C  
583 temperature it's growth increased by 30 % but was reduced under elevated temperature alone  
584 (Errera et al., 2014). A combined increase in pCO<sub>2</sub> and temperature enhanced both the growth  
585 and P<sup>B</sup><sub>m</sub> in the dinoflagellate *Heterosigma akashiwo*, whereas in contrast to the present findings,  
586 only pCO<sub>2</sub> alone enhanced these parameters in *P. cordatum* (Fu et al., 2008).

## 587 **5. Implications**

588 Increased biomass, P<sup>B</sup><sub>m</sub> and a community shift to nanophytoplankton under individual increases  
589 in temperature and pCO<sub>2</sub> suggests a potential negative feedback on atmospheric CO<sub>2</sub>, whereby  
590 more CO<sub>2</sub> is removed from the ocean, and hence from the atmosphere through an increase in  
591 photosynthesis. The selection of *Phaeocystis* spp. under elevated pCO<sub>2</sub> indicates the potential for  
592 negative impacts on ecosystem function and food web structure due to the formation of hypoxic  
593 zones which can occur under eutrophication, inhibitory feeding effects and lowered fecundity in  
594 many copepods associated with this species (Schoemann et al., 2005; Verity et al., 2007). While  
595 more CO<sub>2</sub> is fixed, selection for nanophytoplankton in both of these treatments however, may  
596 result in reduced carbon sequestration due to slower sinking rates of the smaller phytoplankton  
597 cells (Bopp et al., 2001; Laws et al., 2000). When temperature and pCO<sub>2</sub> were elevated  
598 simultaneously, community biomass showed little response and no effects on P<sup>B</sup><sub>m</sub> were  
599 observed. This suggests no change on feedback to atmospheric CO<sub>2</sub> and climate warming in  
600 future warmer high CO<sub>2</sub> oceans. Additionally, combined elevated pCO<sub>2</sub> and temperature  
601 significantly modified taxonomic composition, by reducing diatom biomass relative to the  
602 control with an increase in dinoflagellate biomass dominated by the HAB species, *P. cordatum*.  
603 This has implications for fisheries, ecosystem function and human health.

## 604 **6. Conclusion**

605 These experimental results provide new evidence that increases in pCO<sub>2</sub> coupled with rising sea  
606 temperatures may have antagonistic effects on the autumn phytoplankton community in the  
607 WEC. Under future global change scenarios, the size range and biomass of diatoms may be  
608 reduced with increased dinoflagellate biomass and the selection of HAB species. The  
609 experimental simulations of year 2100 temperature and pCO<sub>2</sub> demonstrate that the effects of  
610 warming can be offset by elevated pCO<sub>2</sub>, maintaining current levels of coastal phytoplankton  
611 productivity while significantly altering the community structure, and in turn these shifts will  
612 have consequences on carbon biogeochemical cycling in the WEC.

613 **Data availability:** Experimental data used for analysis will be made available (DOI will be  
614 created)

615 **Author contributions:** Matthew Keys collected, measured, processed and analysed the data and  
616 prepared the figures. Drs Gavin Tilstone and Helen Findlay conceived, directed and sought the  
617 necessary funds to support the research. Matthew Keys and Dr Gavin Tilstone wrote the paper  
618 with input from Claire Widdicombe and Professor Tracy Lawson. Claire Widdicombe supervised  
619 and advised on phytoplankton taxonomic classifications.

620 **Competing interests:** The authors declare that they have no conflict of interest.

621 **Acknowledgements:** G.H.T, H.S.F. and C.E.W were supported by the UK Natural Environment  
622 Research Council's (NERC) National Capability – The Western English Channel Observatory  
623 (WCO). C.E.W was also partly funded by the NERC and Department for Environment, Food and  
624 Rural Affairs, Marine Ecosystems Research Program (Grant no. NE/L003279/1). M.K. was  
625 supported by a NERC PhD studentship (grant No. NE/L50189X/1). We thank Glen Tarran for his  
626 training, help and assistance with flow cytometry, The National Earth Observation Data Archive  
627 and Analysis Service UK (NEODAAS) for providing the MODIS image used in Fig 1. and the crew  
628 of RV Plymouth Quest for their helpful assistance during field sampling.

## 629 **References**

630 Alley, D., Berntsen, T., Bindoff, N. L., Chen, Z. L., Chidthaisong, A., Friedlingstein, P., Gregory, J., G.,  
631 H., Heimann, M., Hewitson, B., Hoskins, B., Joos, F., Jouzel, Kattsov, V., Lohmann, U., Manning, M.,  
632 Matsuno, T., Molina, M., Nicholls, N., Overpeck, J., Qin, D.H., Raga, G. Ramaswamy, V., Ren, J.W.,  
633 Rusticucci, M., Solomon, S. and Somerville, R., Stocker, T.F., Stott, P., Stouffer, R.J. Whetton, P.,  
634 Wood, R.A. & Wratt, D.: Climate Change 2007. The Physical Science basis: Summary for  
635 policymakers. Contribution of Working Group I to the Fourth Assessment Report of the  
636 Intergovernmental Panel on Climate Change, in ... Climate Change 2007. The Physical Science

637 Basis, Summary for Policy Makers.... [online] Available from:  
638 <http://scholar.google.com/scholar?hl=en&btnG=Search&q=intitle:Climate+Change+2007+:+The+Physical+Science+Basis+Summary+for+Policymakers+Contribution+of+Working+Group+I+to+the+Fourth+Assessment+Report+of+the#3> (Accessed 24 October 2013), 2007.

641 Atkinson, D., Ciotti, B. J. and Montagnes, D. J. S.: Protists decrease in size linearly with  
642 temperature: ca. 2.5% C<sup>-1</sup>, *Proc. R. Soc. B Biol. Sci.*, 270(1533), 2605–2611,  
643 doi:10.1098/rspb.2003.2538, 2003.

644 Badger, M. R., Andrews, T. J., Whitney, S. M., Ludwig, M., Yellowlees, D. C., Leggat, W. and Price, G.  
645 D.: The diversity and coevolution of Rubisco , plastids , pyrenoids , and chloroplast-based CO<sub>2</sub> -  
646 concentrating mechanisms in algae 1, *Can. J. Bot.*, (76), 1052–1071, 1998.

647 Baragi, L. V., Khandeparker, L. and Anil, A. C.: Influence of elevated temperature and pCO<sub>2</sub> on the  
648 marine periphytic diatom *Navicula distans* and its associated organisms in culture,  
649 *Hydrobiologia*, 762(1), 127–142, doi:10.1007/s10750-015-2343-9, 2015.

650 Barnes, M. K., Tilstone, G. H., Smyth, T. J., Widdicombe, C. E., Gloël, J., Robinson, C., Kaiser, J. and  
651 Suggett, D. J.: Drivers and effects of *Karenia mikimotoi* blooms in the western English Channel,  
652 *Prog. Oceanogr.*, 137, 456–469, doi:10.1016/j.pcean.2015.04.018, 2015.

653 Beardall, J., Stojkovic, S. and Larsen, S.: Living in a high CO<sub>2</sub> world: impacts of global climate  
654 change on marine phytoplankton, *Plant Ecol. Divers.*, 2(2), 191–205,  
655 doi:10.1080/17550870903271363, 2009.

656 Bermúdez, J. R., Riebesell, U., Larsen, A. and Winder, M.: Ocean acidification reduces transfer of  
657 essential biomolecules in a natural plankton community, *Sci. Rep.*, 6(1), 27749,  
658 doi:10.1038/srep27749, 2016.

659 Booth, B. C.: Size classes and major taxonomic groups of phytoplankton at two locations in the  
660 subarctic pacific ocean in May and August, 1984, *Mar. Biol.*, 97(2), 275–286,  
661 doi:10.1007/BF00391313, 1988.

662 Bopp, L. , Monfray, P. , Aumont, O. , Dufresne, J.-L. , Le Treut, H. , Madec, G. , Terray, L. . and  
663 Orr, J. C. .: Potential impact of climate change on marine export production, *Global Biogeochem.*  
664 *Cycles*, 15(1), 81–99, doi:10.1029/1999GB001256, 2001.

665 Boras, J. A., Borrull, E., Cardelu, C., Cros, L., Gomes, A., Sala, M. M., Aparicio, F. L., Balague, V.,  
666 Mestre, M., Movilla, J., Sarmiento, H., Va, E. and Lo, A.: Contrasting effects of ocean acidification on  
667 the microbial food web under different trophic conditions, *ICES J. Mar. Sci.*, 73(73 (3)), 670–679,  
668 2016.

669 Boyd, P. W. and Doney, S. C.: Modelling regional responses by marine pelagic ecosystems to  
670 global climate change, *Geophys. Res. Lett.*, 29(16), 1–4, 2002.

671 Boyd, P. W., Rynearson, T. A., Armstrong, E. A., Fu, F., Hayashi, K., Hu, Z., Hutchins, D. A., Kudela,  
672 R. M., Litchman, E., Mulholland, M. R., Passow, U., Strzepek, R. F., Whittaker, K. A., Yu, E. and  
673 Thomas, M. K.: Marine Phytoplankton Temperature versus Growth Responses from Polar to  
674 Tropical Waters - Outcome of a Scientific Community-Wide Study, *PLoS One*, 8(5),  
675 doi:10.1371/journal.pone.0063091, 2013.

676 Brussaard, C. P. D., Noordeloos, A. A. M., Witte, H., Collenteur, M. C. J., Schulz, K., Ludwig, A. and  
677 Riebesell, U.: Arctic microbial community dynamics influenced by elevated CO<sub>2</sub> levels,  
678 *Biogeosciences*, 10(2), 719–731, doi:10.5194/bg-10-719-2013, 2013.

679 Calbet, A., Sazhin, A. F., Nejstgaard, J. C., Berger, S. a, Tait, Z. S., Olmos, L., Sousoni, D., Isari, S.,  
680 Martínez, R. a, Bouquet, J.-M., Thompson, E. M., Båmstedt, U. and Jakobsen, H. H.: Future climate  
681 scenarios for a coastal productive planktonic food web resulting in microplankton phenology  
682 changes and decreased trophic transfer efficiency., *PLoS One*, 9(4), e94388,  
683 doi:10.1371/journal.pone.0094388, 2014.

684 Chen, S., Beardall, J. and Gao, K.: A red tide alga grown under ocean acidification upregulates its  
685 tolerance to lower pH by increasing its photophysiological functions, *Biogeosciences*, 11, 4829–  
686 4837, doi:10.5194/bg-11-4829-2014, 2014.

687 Coello-Camba, A. and Agustí, S.: Acidification counteracts negative effects of warming on diatom  
688 silicification, *Biogeosciences Discuss.*, 30(October), 1–19, doi:10.5194/bg-2016-424, 2016.

689 Coello-Camba, A., Agustí, S., Holding, J., Arrieta, J. M. and Duarte, C. M.: Interactive effect of  
690 temperature and CO<sub>2</sub> increase in Arctic phytoplankton, *Front. Mar. Sci.*,  
691 1(October), 1–10, doi:10.3389/fmars.2014.00049, 2014.

692 Delille, B., Harlay, J., Zondervan, I., Jacquet, S., Chou, L., Wollast, R., Bellerby, R. G. J.,  
693 Frankignoulle, M., Borges, A. V., Riebesell, U. and Gattuso, J.-P.: Response of primary production  
694 and calcification to changes of p CO<sub>2</sub> during experimental blooms of the coccolithophorid  
695 *Emiliana huxleyi*, *Global Biogeochem. Cycles*, 19(2), n/a-n/a, doi:10.1029/2004GB002318,  
696 2005.

697 Deppeler, S. L. and Davidson, A. T.: Southern Ocean Phytoplankton in a Changing Climate, *Front.*  
698 *Mar. Sci.*, 4(February), doi:10.3389/fmars.2017.00040, 2017.

699 Dickson, A. G. and Millero, F. J.: A comparison of the equilibrium constants for the dissociation of  
700 carbonic acid in seawater media, *Deep Sea Res. Part I Oceanogr. Res. Pap.*, 34(111), 1733–1743,

701 1987.

702 Dunne, J. P.: A roadmap on ecosystem change, *Nat. Clim. Chang.*, 5, 20 [online] Available from:  
703 <http://dx.doi.org/10.1038/nclimate2480>, 2014.

704 Edwards, M., Johns, D., Leterme, S. C., Svendsen, E. and Richardson, A. J.: Regional climate change  
705 and harmful algal blooms in the northeast Atlantic, *Limnol. Oceanogr.*, 51(2), 820–829,  
706 doi:10.4319/lo.2006.51.2.0820, 2006.

707 Eilertsen, H. and Raa, J.: Toxins in seawater produced by a common phytoplankter : *phaeocystis*  
708 *pouchetii*, *J. Mar. Biotechnol.*, 3(1), 115–119 [online] Available from:  
709 <http://ci.nii.ac.jp/naid/10002209414/en/> (Accessed 28 January 2016), 1995.

710 Engel, A., Schulz, K. G., Riebesell, U., Bellerby, R., Delille, B. and Schartau, M.: Effects of CO<sub>2</sub> on  
711 particle size distribution and phytoplankton abundance during a mesocosm bloom experiment  
712 (PeECE II), *Biogeosciences*, 5, 509–521, doi:10.5194/bgd-4-4101-2007, 2008.

713 Eppley, R. W.: Temperature and phytoplankton growth in the sea, *Fish. Bull.*, 70(4), 1063–1085,  
714 1972.

715 Errera, R. M., Yvon-Lewis, S., Kessler, J. D. and Campbell, L.: Responses of the dinoflagellate  
716 *Karenia brevis* to climate change: pCO<sub>2</sub> and sea surface temperatures, *Harmful Algae*, 37, 110–  
717 116, doi:10.1016/j.hal.2014.05.012, 2014.

718 Feng, Y., Warner, M. E., Zhang, Y., Sun, J., Fu, F.-X., Rose, J. M. and Hutchins, D. a.: Interactive  
719 effects of increased pCO<sub>2</sub>, temperature and irradiance on the marine coccolithophore *Emiliana*  
720 *huxleyi* (Prymnesiophyceae), *Eur. J. Phycol.*, 43(1), 87–98, doi:10.1080/09670260701664674,  
721 2008.

722 Feng, Y., Hare, C., Leblanc, K., Rose, J., Zhang, Y., DiTullio, G., Lee, P., Wilhelm, S., Rowe, J., Sun, J.,  
723 Nemcek, N., Gueguen, C., Passow, U., Benner, I., Brown, C. and Hutchins, D.: Effects of increased  
724 pCO<sub>2</sub> and temperature on the North Atlantic spring bloom. I. The phytoplankton community  
725 and biogeochemical response, *Mar. Ecol. Prog. Ser.*, 388, 13–25, doi:10.3354/meps08133, 2009.

726 Fu, F.-X., Warner, M. E., Zhang, Y., Feng, Y. and Hutchins, D. a.: Effects of Increased Temperature  
727 and Co<sub>2</sub> on Photosynthesis, Growth, and Elemental Ratios in Marine *Synechococcus* and  
728 *Prochlorococcus* (Cyanobacteria), *J. Phycol.*, 43(3), 485–496, doi:10.1111/j.1529-  
729 8817.2007.00355.x, 2007a.

730 Fu, F.-X., Warner, M. E., Zhang, Y., Feng, Y. and Hutchins, D. a.: Effects of Increased Temperature  
731 and Co<sub>2</sub> on Photosynthesis, Growth, and Elemental Ratios in Marine *Synechococcus* and  
732 *Prochlorococcus* (Cyanobacteria), *J. Phycol.*, 43(3), 485–496, doi:10.1111/j.1529-

733 8817.2007.00355.x, 2007b.

734 Fu, F.-X., Zhang, Y., Warner, M. E., Feng, Y., Sun, J. and Hutchins, D. a.: A comparison of future  
735 increased CO<sub>2</sub> and temperature effects on sympatric *Heterosigma akashiwo* and *Prorocentrum*  
736 *minimum*, *Harmful Algae*, 7(1), 76–90, doi:10.1016/j.hal.2007.05.006, 2008.

737 Gao, G., Jin, P., Liu, N., Li, F., Tong, S., Hutchins, D. A. and Gao, K.: The acclimation process of  
738 phytoplankton biomass, carbon fixation and respiration to the combined effects of elevated  
739 temperature and pCO<sub>2</sub> in the northern South China Sea, *Mar. Pollut. Bull.*, 118(1–2), 213–220,  
740 doi:10.1016/j.marpolbul.2017.02.063, 2017.

741 Giordano, M., Beardall, J. and Raven, J. a: CO<sub>2</sub> concentrating mechanisms in algae: mechanisms,  
742 environmental modulation, and evolution., *Annu. Rev. Plant Biol.*, 56(January), 99–131,  
743 doi:10.1146/annurev.arplant.56.032604.144052, 2005.

744 Goldman, J. and Carpenter, E.: A kinetic approach to the effect of temperature on algal growth,  
745 *Limnol. Oceanogr.*, 19(5), 756–766, doi:10.4319/lo.1974.19.5.0756, 1974.

746 Hansen, P.: Effect of high pH on the growth and survival of marine phytoplankton: implications  
747 for species succession, *Aquat. Microb. Ecol.*, 28, 279–288, doi:10.3354/ame028279, 2002.

748 Hare, C., Leblanc, K., DiTullio, G., Kudela, R., Zhang, Y., Lee, P., Riseman, S. and Hutchins, D.:  
749 Consequences of increased temperature and CO<sub>2</sub> for phytoplankton community structure in the  
750 Bering Sea, *Mar. Ecol. Prog. Ser.*, 352, 9–16, doi:10.3354/meps07182, 2007a.

751 Hare, C., Leblanc, K., DiTullio, G., Kudela, R., Zhang, Y., Lee, P., Riseman, S. and Hutchins, D.:  
752 Consequences of increased temperature and CO<sub>2</sub> for phytoplankton community structure in the  
753 Bering Sea, *Mar. Ecol. Prog. Ser.*, 352, 9–16, doi:10.3354/meps07182, 2007b.

754 Hinga, K. R.: Effects of pH on coastal marine phytoplankton, *Mar. Ecol. Prog. Ser.*, 238, 281–300,  
755 2002.

756 Hoogstraten, a., Peters, M., Timmermans, K. R. and De Baar, H. J. W.: Combined effects of  
757 inorganic carbon and light on *Phaeocystis globosa* Scherffel (*Prymnesiophyceae*),  
758 *Biogeosciences*, 9(5), 1885–1896, doi:10.5194/bg-9-1885-2012, 2012.

759 Hutchins, D. a., Fu, F.-X., Zhang, Y., Warner, M. E., Feng, Y., Portune, K., Bernhardt, P. W. and  
760 Mulholland, M. R.: CO<sub>2</sub> control of *Trichodesmium* N<sub>2</sub> fixation, photosynthesis, growth rates, and  
761 elemental ratios: Implications for past, present, and future ocean biogeochemistry, *Limnol.*  
762 *Oceanogr.*, 52(4), 1293–1304, doi:10.4319/lo.2007.52.4.1293, 2007.

763 Ipcc: Climate Change 2013: The Physical Science Basis. Contribution of Working Group I to the

764 Fifth Assessment Report of the Intergovernmental Panel on Climate Change, Intergov. Panel  
765 Clim. Chang. Work. Gr. I Contrib. to IPCC Fifth Assess. Rep. (AR5)(Cambridge Univ Press. New  
766 York), 1535, doi:10.1029/2000JD000115, 2013.

767 Keys, M.: "Effects of future CO<sub>2</sub> and temperature regimes on phytoplankton community  
768 composition, biomass and photosynthetic rates in the Western English Channel", PhD thesis.,  
769 University of Essex, United Kingdom., 2017.

770 Keys, M., Tilstone, G., Findlay, H. S., Widdicombe, C. E. and Lawson, T.: Effects of elevated CO<sub>2</sub> on  
771 phytoplankton community biomass and species composition during a spring *Phaeocystis* spp.  
772 bloom in the western English Channel, *Harmful Algae*, 67, 92–106,  
773 doi:10.1016/j.hal.2017.06.005, 2017.

774 Kiefer, D. a. and Mitchell, B. G.: A simple steady state description of phytoplankton growth based  
775 on absorption cross section and quantum efficiency, *Limnol. Oceanogr.*, 28(4), 770–776,  
776 doi:10.4319/lo.1983.28.4.0770, 1983.

777 Kim, J.-M., Lee, K., Shin, K., Kang, J.-H., Lee, H.-W., Kim, M., Jang, P.-G. and Jang, M.-C.: The effect of  
778 seawater CO<sub>2</sub> concentration on growth of a natural phytoplankton assemblage in a controlled  
779 mesocosm experiment, *Limnol. Oceanogr.*, 51(4), 1629–1636, doi:10.4319/lo.2006.51.4.1629,  
780 2006a.

781 Kim, J.-M., Lee, K., Shin, K., Kang, J.-H., Lee, H.-W., Kim, M., Jang, P.-G. and Jang, M.-C.: The effect of  
782 seawater CO<sub>2</sub> concentration on growth of a natural phytoplankton assemblage in a controlled  
783 mesocosm experiment, *Limnol. Oceanogr.*, 51(4), 1629–1636, doi:10.4319/lo.2006.51.4.1629,  
784 2006b.

785 Kitidis, V., Hardman-mountford, N. J., Litt, E., Brown, I., Cummings, D., Hartman, S., Hydes, D.,  
786 Fishwick, J. R., Harris, C., Martinez-vicente, V., Woodward, E. M. S. and Smyth, T. J.: Seasonal  
787 dynamics of the carbonate system in the Western English Channel, *Cont. Shelf Res.*, 42, 2–12,  
788 2012.

789 Kolber, Z. S., Prášil, O. and Falkowski, P. G.: Measurements of variable chlorophyll fluorescence  
790 using fast repetition rate techniques: Defining methodology and experimental protocols,  
791 *Biochim. Biophys. Acta - Bioenerg.*, 1367(1–3), 88–106, doi:10.1016/S0005-2728(98)00135-2,  
792 1998.

793 Lawrenz, E., Silsbe, G., Capuzzo, E., Ylöstalo, P., Forster, R. M., Simis, S. G. H., Prášil, O.,  
794 Kromkamp, J. C., Hickman, A. E., Moore, C. M., Forget, M. H., Geider, R. J. and Suggett, D. J.:  
795 Predicting the Electron Requirement for Carbon Fixation in Seas and Oceans, *PLoS One*, 8(3),  
796 doi:10.1371/journal.pone.0058137, 2013.



797 Laws, E. A., Falkowski, P. G., Smith, W. O., Ducklow, H. W. and McCarthy, J. J.: Temperature effects  
798 on export production in the open ocean, *Global Biogeochem. Cycles*, 14(4), 1231–1246,  
799 doi:10.1029/1999GB001229, 2000.

800 Li, W. K. W., McLaughlin, F. A., Lovejoy, C. and Carmack, E. C.: Smallest Algae Thrive As the Arctic  
801 Ocean Freshens, *Science* (80-. ), 326(5952), 539–539, doi:10.1126/science.1179798, 2009.

802 Lomas, M. W. and Glibert, P. M.: Interactions between NH<sub>4</sub><sup>+</sup> and NO<sub>3</sub><sup>-</sup> uptake and  
803 assimilation: Comparison of diatoms and dinoflagellates at several growth temperatures, *Mar.*  
804 *Biol.*, 133(3), 541–551, doi:10.1007/s002270050494, 1999.

805 Love, B. A., Olson, M. B. and Wuori, T.: Technical Note: A minimally-invasive experimental  
806 system for pCO<sub>2</sub> manipulation in plankton cultures  
807 using passive gas exchange (Atmospheric Carbon Control Simulator), *Biogeosciences Discuss.*,  
808 (December), 1–19, doi:10.5194/bg-2016-502, 2016.

809 Matear, R. J. and Lenton, A.: Carbon–climate feedbacks accelerate ocean acidification,  
810 *Biogeosciences*, 15(6), 1721–1732, doi:10.5194/bg-15-1721-2018, 2018.

811 Maugendre, L., Gattuso, J. P., Poulton, A. J., Dellisanti, W., Gaubert, M., Guieu, C. and Gazeau, F.: No  
812 detectable effect of ocean acidification on plankton metabolism in the NW oligotrophic  
813 Mediterranean Sea: Results from two mesocosm studies, *Estuar. Coast. Shelf Sci.*, 186, 89–99,  
814 doi:10.1016/j.ecss.2015.03.009, 2017.

815 Mehrbach, C., Culberson, C. H., Hawley, J. E. and Pytkowicz, R. M.: Measurement of the Apparent  
816 Dissociation Constants of Carbonic Acid in Seawater at Atmospheric Pressure, *Limnol.*  
817 *Oceanogr.*, 18(1932), 897–907, 1973.

818 Menden-Deuer, S. and Lessard, E. J.: Carbon to volume relationships for dinoflagellates, diatoms,  
819 and other protist plankton, *Limnol. Oceanogr.*, 45(3), 569–579, doi:10.4319/lo.2000.45.3.0569,  
820 2000.

821 Morán, X. A. G., López-Urrutia, Á., Calvo-Díaz, A. and Li, W. K. W.: Increasing importance of small  
822 phytoplankton in a warmer ocean, *Glob. Chang. Biol.*, 16(3), 1137–1144, doi:10.1111/j.1365-  
823 2486.2009.01960.x, 2010.

824 Morse, D., Salois, P., Markovic, P. and Hastings, J. W.: A nuclear-encoded form II RuBisCO in  
825 dinoflagellates., *Science*, 268(5217), 1622–1624, doi:10.1126/science.7777861, 1995.

826 Moustaka-Gouni, M., Kormas, K. A., Scotti, M., Vardaka, E. and Sommer, U.: Warming and  
827 Acidification Effects on Planktonic Heterotrophic Pico- and Nanoflagellates in a Mesocosm  
828 Experiment, *Protist*, 167(4), 389–410, doi:10.1016/j.protis.2016.06.004, 2016.

829 Oxborough, K., Moore, C. M., Suggett, D. J., Lawson, T., Chan, H. G. and Geider, R. J.: Direct  
830 estimation of functional PSII reaction center concentration and PSII electron flux on a volume  
831 basis: a new approach to the analysis of Fast Repetition Rate fluorometry (FRRf) data, *Limnol.*  
832 *Oceanogr. Methods*, 10, 142–154, doi:10.4319/lom.2012.10.142, 2012.

833 Paul, C., Matthiessen, B. and Sommer, U.: Warming, but not enhanced CO<sub>2</sub> concentration,  
834 quantitatively and qualitatively affects phytoplankton biomass, *Mar. Ecol. Prog. Ser.*, 528, 39–51,  
835 doi:10.3354/meps11264, 2015.

836 Paulino, a. I., Egge, J. K. and Larsen, a.: Effects of increased atmospheric CO<sub>2</sub> on small and  
837 intermediate sized osmotrophs during a nutrient induced phytoplankton bloom, *Biogeosciences*  
838 *Discuss.*, 4(6), 4173–4195, doi:10.5194/bgd-4-4173-2007, 2007.

839 Peter, K. H. and Sommer, U.: Phytoplankton Cell Size: Intra- and Interspecific Effects of  
840 Warming and Grazing, *PLoS One*, 7(11), doi:10.1371/journal.pone.0049632, 2012.

841 Pierrot, D., Lewis, E. and Wallace, D. W. R.: MS Excel program developed for CO<sub>2</sub> system  
842 calculations, ORNL/CDIAC-105a. Carbon Dioxide Inf. Anal. Center, Oak Ridge Natl. Lab. US Dep.  
843 Energy, Oak Ridge, Tennessee, 2006.

844 Raupach, M. R., Marland, G., Ciais, P., Le Quéré, C., Canadell, J. G., Klepper, G. and Field, C. B.:  
845 Global and regional drivers of accelerating CO<sub>2</sub> emissions., *Proc. Natl. Acad. Sci. U. S. A.*, 104(24),  
846 10288–93, doi:10.1073/pnas.0700609104, 2007.

847 Raven, J., Caldeira, K., Elderfield, H., H.-G. and others: Ocean acidification due to increasing  
848 atmospheric carbon dioxide, *R. Soc.*, (June), 2005.

849 Raven, J. A. and Geider, R. J.: Temperature and algal growth, *New Phytol.*, 110(4), 441–461,  
850 doi:10.1111/j.1469-8137.1988.tb00282.x, 1988.

851 Reinfelder, J. R.: Carbon Concentrating Mechanisms in Eukaryotic Marine Phytoplankton, *Ann.*  
852 *Rev. Mar. Sci.*, 3(1), 291–315, doi:10.1146/annurev-marine-120709-142720, 2011.

853 Riebesell, U.: Effects of CO<sub>2</sub> Enrichment on Marine Phytoplankton, *J. Oceanogr.*, 60(4), 719–729,  
854 doi:10.1007/s10872-004-5764-z, 2004.

855 Riebesell, U., Schulz, K. G., Bellerby, R. G. J., Botros, M., Fritsche, P., Meyerhöfer, M., Neill, C.,  
856 Nondal, G., Oschlies, a, Wohlers, J. and Zöllner, E.: Enhanced biological carbon consumption in a  
857 high CO<sub>2</sub> ocean., *Nature*, 450(7169), 545–8, doi:10.1038/nature06267, 2007.

858 Riebesell, U., Fabry, V. J., Hansson, L. and Gattuso, J.-P.: Guide to best practices for ocean  
859 acidification, edited by L. H. and J. -P. G. L. U. Riebesell, V. J. Fabry, Publications Office Of The

860 European Union., 2010.

861 Rost, B., Riebesell, U., Burkhardt, S. and Su, D.: Carbon acquisition of bloom-forming marine  
862 phytoplankton, *Limnol. Oceanogr.*, 48(1), 55–67, 2003.

863 Sathyendranath, S., Stuart, V., Nair, A., Oka, K., Nakane, T., Bouman, H., Forget, M. H., Maass, H.  
864 and Platt, T.: Carbon-to-chlorophyll ratio and growth rate of phytoplankton in the sea, *Mar. Ecol.  
865 Prog. Ser.*, 383, 73–84, doi:10.3354/meps07998, 2009.

866 Savage, V. M., Gillooly, J. F., Brown, J. H., West, G. B. and Charnov, E. L.: Effects of Body Size and  
867 Temperature on Population Growth, *Am. Nat.*, 163(3), 429–441, doi:10.1086/381872, 2004.

868 Schoemann, V., Becquevort, S., Stefels, J., Rousseau, V. and Lancelot, C.: Phaeocystis blooms in the  
869 global ocean and their controlling mechanisms: a review, *J. Sea Res.*, 53(1–2), 43–66,  
870 doi:10.1016/j.seares.2004.01.008, 2005.

871 Schulz, K. G., Ramos, J. B., Zeebe, R. E. and Riebesell, U.: Biogeosciences CO<sub>2</sub> perturbation  
872 experiments : similarities and differences between dissolved inorganic carbon and total  
873 alkalinity manipulations, *Biogeosciences*, 6, 2145–2153, 2009.

874 Shi, D., Xu, Y. and Morel, F. M. M.: Effects of the pH/*p*CO<sub>2</sub> control method on medium chemistry  
875 and phytoplankton growth, *Biogeosciences*, 6(7), 1199–1207, doi:10.5194/bg-6-1199-2009,  
876 2009.

877 Smetacek, V. and Cloern, J. E.: On Phytoplankton Trends, *Science* (80-. ), 319(5868), 1346–1348  
878 [online] Available from: <http://www.jstor.org/stable/20053523>, 2008.

879 Smyth, T. J., Fishwick, J. R., AL-Moosawi, L., Cummings, D. G., Harris, C., Kitidis, V., Rees, A.,  
880 Martinez-Vicente, V. and Woodward, E. M. S.: A broad spatio-temporal view of the Western  
881 English Channel observatory, *J. Plankton Res.*, 32(5), 585–601, doi:10.1093/plankt/fbp128,  
882 2010.

883 Strom, S.: Novel interactions between phytoplankton and microzooplankton : their influence on  
884 the coupling between growth and grazing rates in the sea, , 41–54, 2002.

885 Tarran, G. a., Heywood, J. L. and Zubkov, M. V.: Latitudinal changes in the standing stocks of  
886 nano- and picoeukaryotic phytoplankton in the Atlantic Ocean, *Deep Sea Res. Part II Top. Stud.  
887 Oceanogr.*, 53(14–16), 1516–1529, doi:10.1016/j.dsr2.2006.05.004, 2006.

888 Taucher, J., Jones, J., James, A., Brzezinski, M. A., Carlson, C. A., Riebesell, U. and Passow, U.:  
889 Combined effects of CO<sub>2</sub> and temperature on carbon uptake and partitioning by the marine  
890 diatoms *Thalassiosira weissflogii* and *Dactyliosolen fragilissimus*, *Limnol. Oceanogr.*, 60(3),

891 901–919, doi:10.1002/lno.10063, 2015.

892 Thoisen, C., Riisgaard, K., Lundholm, N., Nielsen, T. and Hansen, P.: Effect of acidification on an  
893 Arctic phytoplankton community from Disko Bay, West Greenland, *Mar. Ecol. Prog. Ser.*, 520,  
894 21–34, doi:10.3354/meps11123, 2015.

895 Thomas, M. K., Kremer, C. T., Klausmeier, C. A. and Litchman, E.: A Global Pattern of Thermal  
896 Adaptation in Marine Phytoplankton, *Science (80-. )*, 338(6110), 1085–1088,  
897 doi:10.1126/science.1224836, 2012.

898 Torstensson, A., Chierici, M. and Wulff, A.: The influence of increased temperature and carbon  
899 dioxide levels on the benthic/sea ice diatom *Navicula directa*, *Polar Biol.*, 35(2), 205–214,  
900 doi:10.1007/s00300-011-1056-4, 2012.

901 Tortell, P., DiTullio, G., Sigman, D. and Morel, F.: CO<sub>2</sub> effects on taxonomic composition and  
902 nutrient utilization in an Equatorial Pacific phytoplankton assemblage, *Mar. Ecol. Prog. Ser.*, 236,  
903 37–43, doi:10.3354/meps236037, 2002.

904 Tortell, P. D., Payne, C. D., Li, Y., Trimborn, S., Rost, B., Smith, W. O., Riesselman, C., Dunbar, R. B.,  
905 Sedwick, P. and DiTullio, G. R.: CO<sub>2</sub> sensitivity of Southern Ocean phytoplankton, *Geophys. Res.*  
906 *Let.*, 35(4), L04605, doi:10.1029/2007GL032583, 2008.

907 Utermöhl, H.: Zur vervollkommnung der quantitativen phytoplankton-methodik, *Mitt. int. Ver.*  
908 *theor. angew. Limnol.*, 9, 1–38, 1958.

909 Verity, P. G., Brussaard, C. P., Nejtgaard, J. C., Van Leeuwe, M. a., Lancelot, C. and Medlin, L. K.:  
910 Current understanding of *Phaeocystis* ecology and biogeochemistry, and perspectives for future  
911 research, edited by M. A. van Leeuwe, J. Stefels, S. Belviso, C. Lancelot, P. G. Verity, and W. W. C.  
912 Gieskes, Springer Netherlands., 2007.

913 Webb, W. L., Newton, M. and Starr, D.: Carbon dioxide exchange of *Alnus rubra*, *Oecologia*, 17(4),  
914 281–291, doi:10.1007/BF00345747, 1974.

915 Welschmeyer: Fluorometric analysis of chlorophyll a in the presence of chlorophyll b and  
916 pheopigments, *Limnol. Oceanogr.*, 39(8), 1985–1992, 1994.

917 Widdicombe, C. E., Eloire, D., Harbour, D., Harris, R. P. and Somerfield, P. J.: Long-term  
918 phytoplankton community dynamics in the Western English Channel, *J. Plankton Res.*, 32(5),  
919 643–655, doi:10.1093/plankt/fbp127, 2010a.

920 Widdicombe, C. E., Eloire, D., Harbour, D., Harris, R. P. and Somerfield, P. J.: Long-term  
921 phytoplankton community dynamics in the Western English Channel, *J. Plankton Res.*, 32(5),

922 643–655, doi:10.1093/plankt/fbp127, 2010b.

923 Wolf-gladrow, B. D. A., Riebesell, U. L. F., Burkhardt, S. and Jelle, B.: Direct effects of CO<sub>2</sub>  
924 concentration on growth and isotopic composition of marine plankton, *Tellus*, 51B, 461–476,  
925 1999.

926 Woods, H. A. and Harrison, J. F.: Temperature and the chemical composition of poikilothermic  
927 organisms, , (Sidell 1998), 237–245, 2003.

928

929

930

931

932

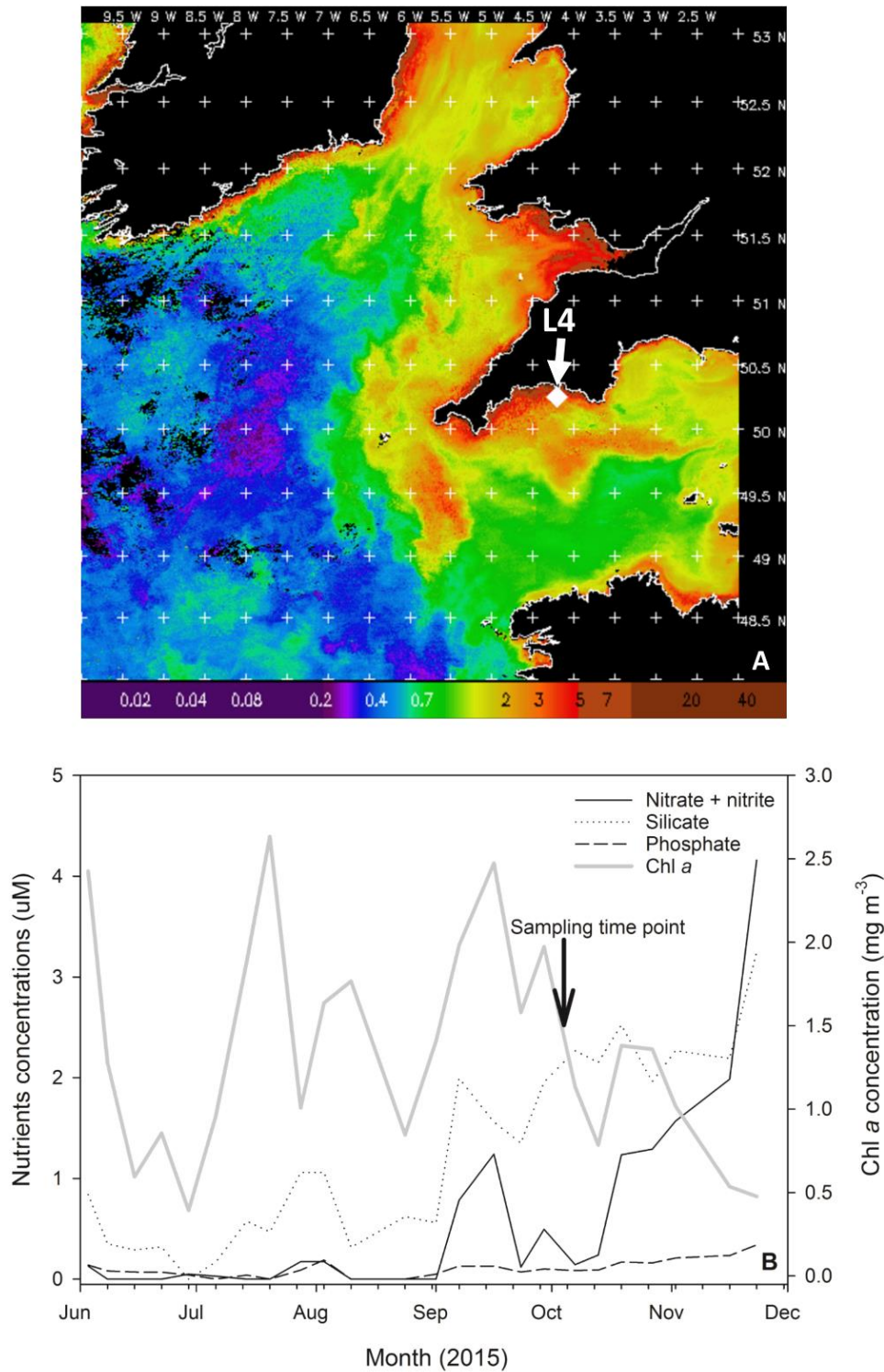


**Fig. 1.** (A). MODIS weekly composite chl *a* image of the western English Channel covering the period 30<sup>th</sup> September – 6<sup>th</sup> October 2015 (coincident with the week of phytoplankton community sampling for the present study), processing courtesy of NEODAAS. The position of coastal station L4 is marked with a white diamond. (B). Profiles of weekly nutrient and chl *a* concentrations from station L4 at a depth of 10 m over the second half of 2015 in the months prior to phytoplankton community sampling (indicated by black arrow and text).

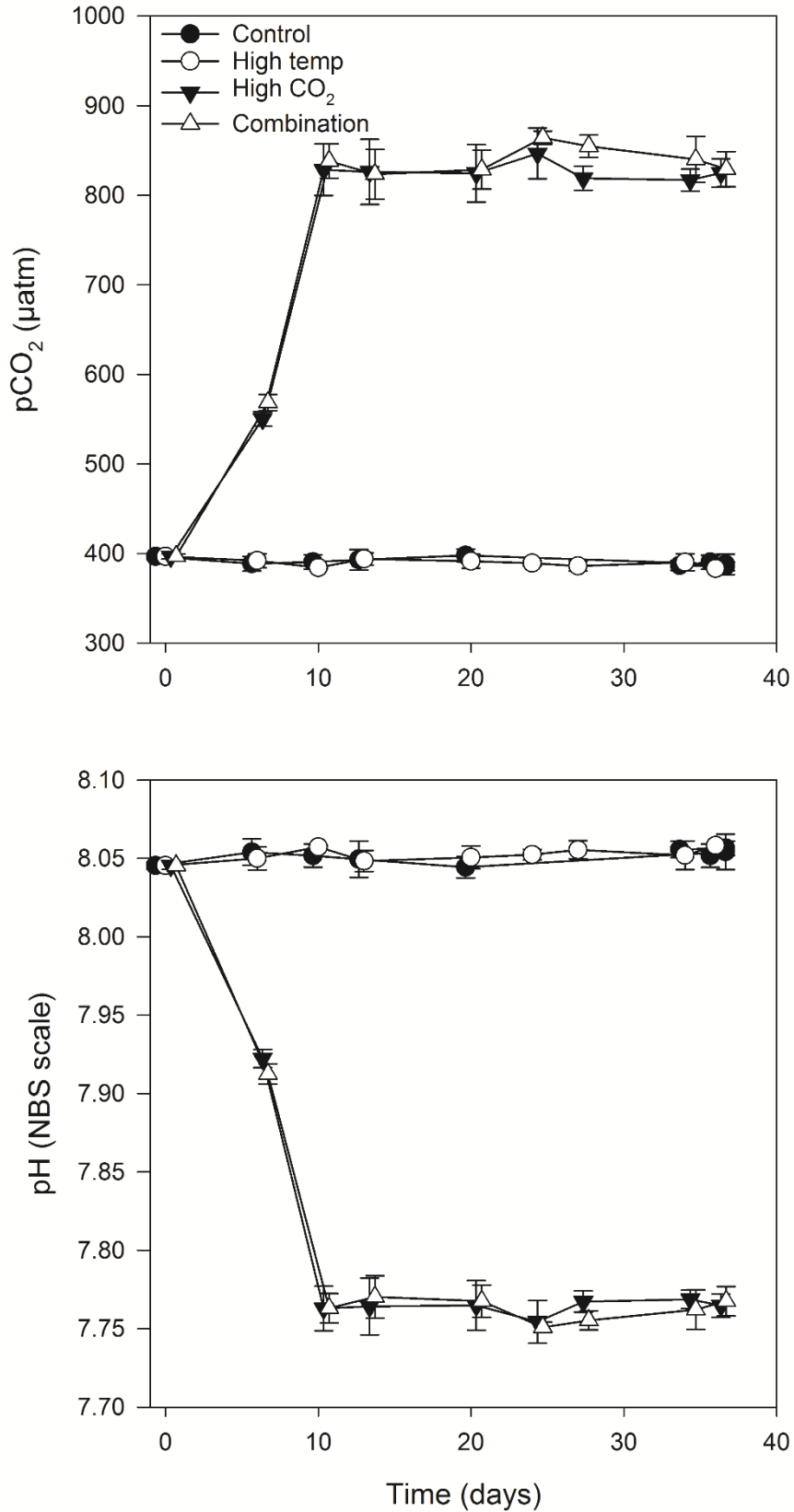


**Fig. 2.** Calculated values of partial pressure of CO<sub>2</sub> in seawater (pCO<sub>2</sub>) (A) and pH (B) from direct measurements of total alkalinity and dissolved inorganic carbon. (For full carbonate system values see **Table S1.**, supplementary material)

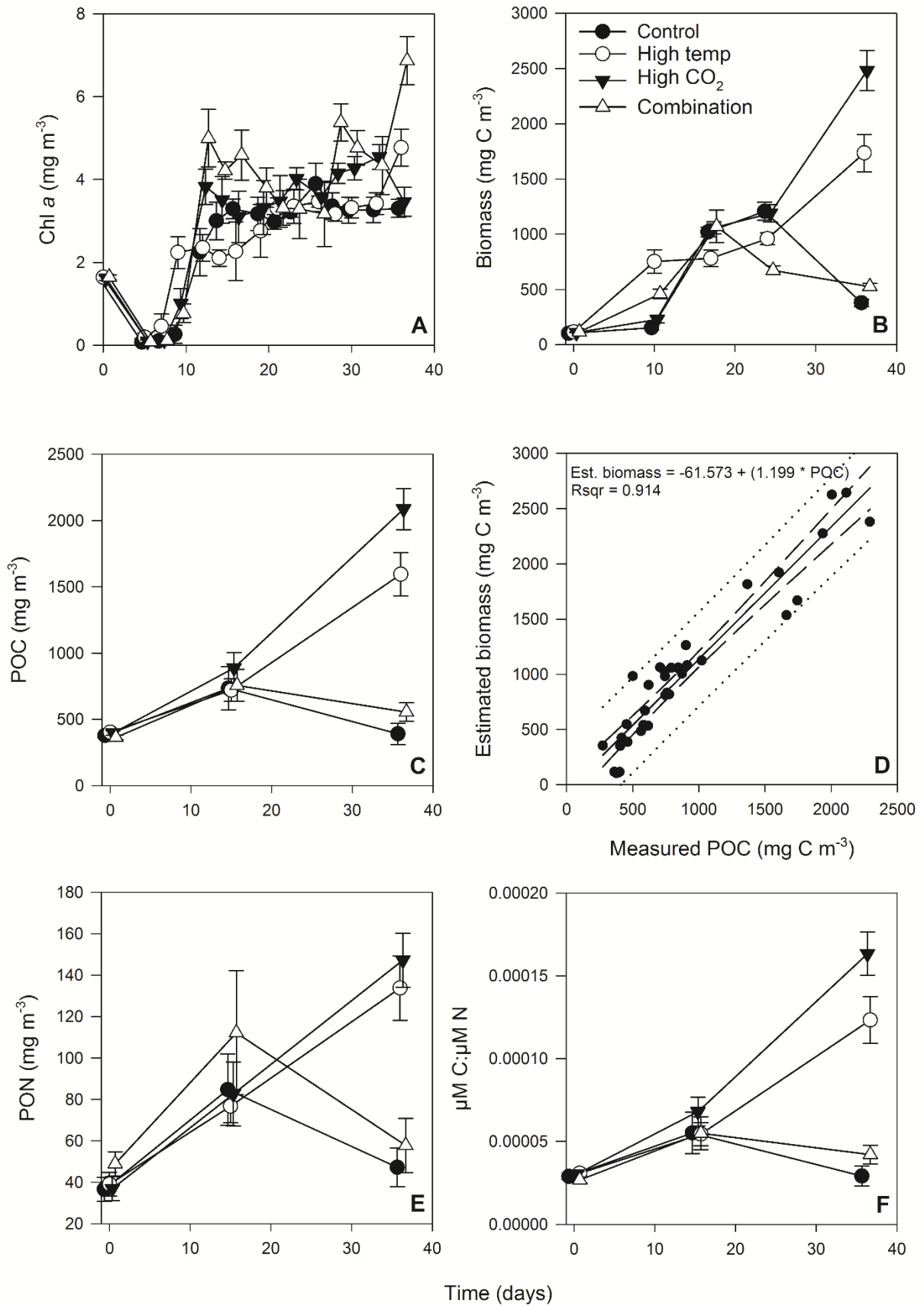


**Fig. 3.** Time course of chl *a* (A), estimated phytoplankton biomass (B), POC (C), regression of estimated phytoplankton carbon vs measured POC (D), PON (E) and POC:PON (F).



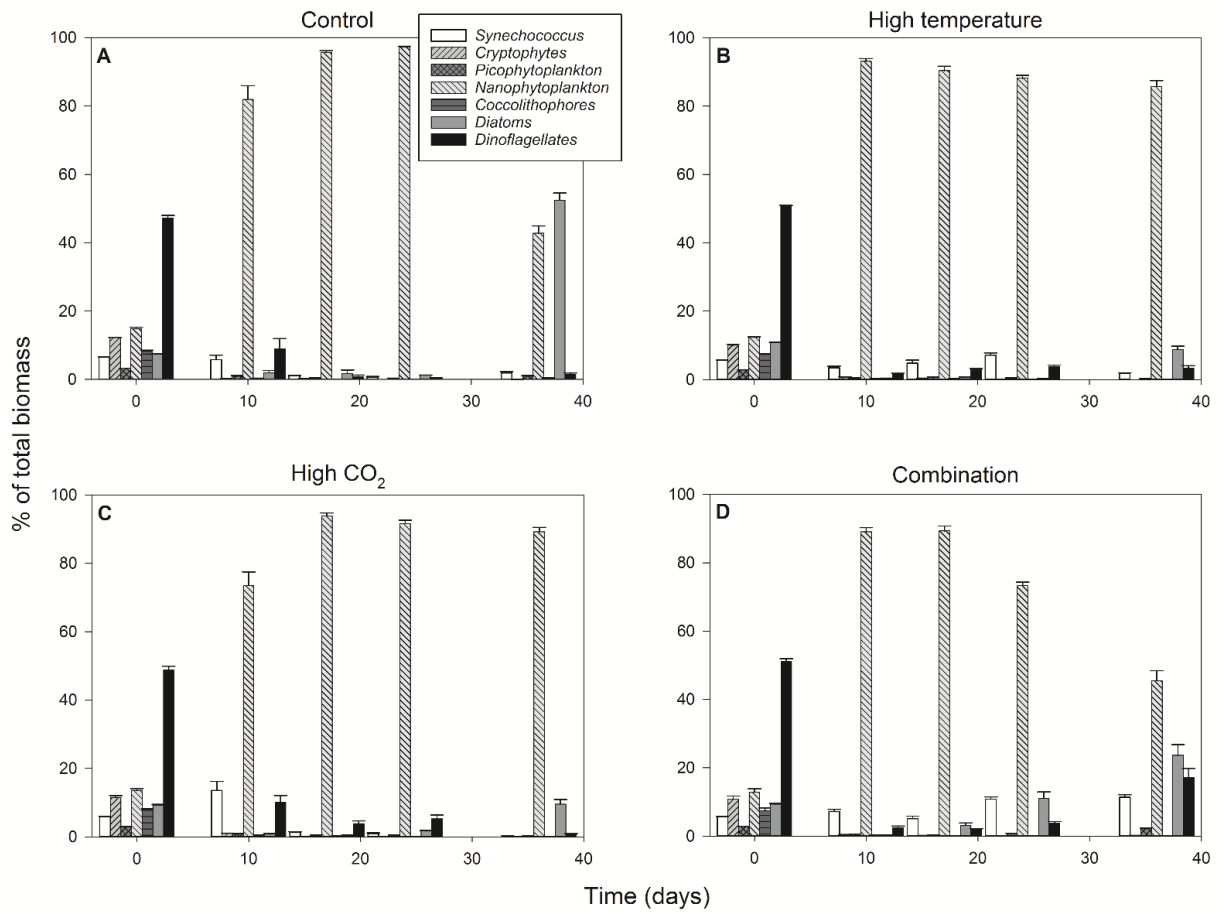


**Fig. 4.** Percentage contribution to community biomass by phytoplankton groups/species throughout the experiment in the control (A), high temperature (B), high CO<sub>2</sub> (C) and combination treatments (D).

936

937

938

939

940

941

942

943

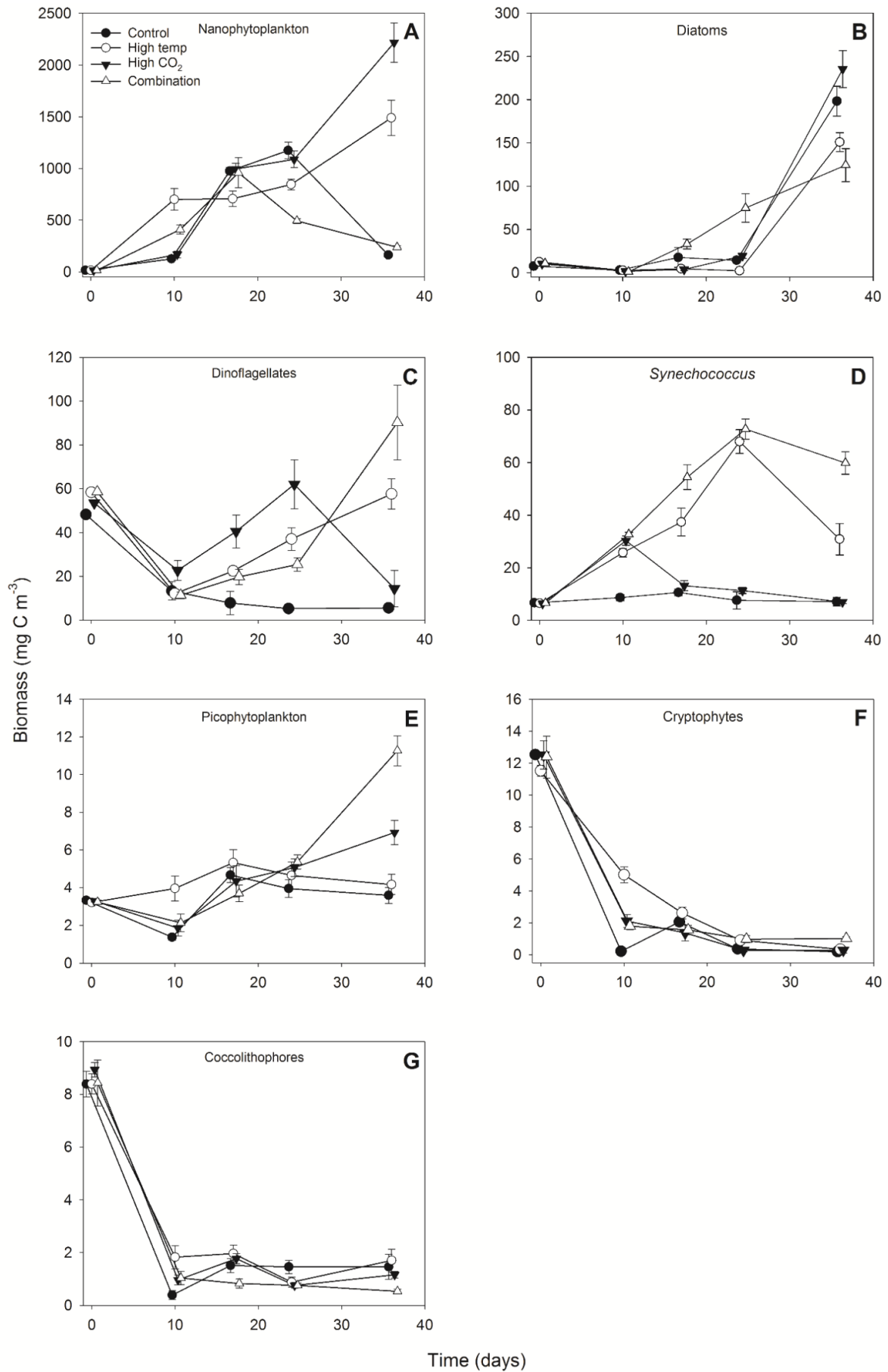


**Fig. 5.** Response of individual phytoplankton groups to experimental treatments.

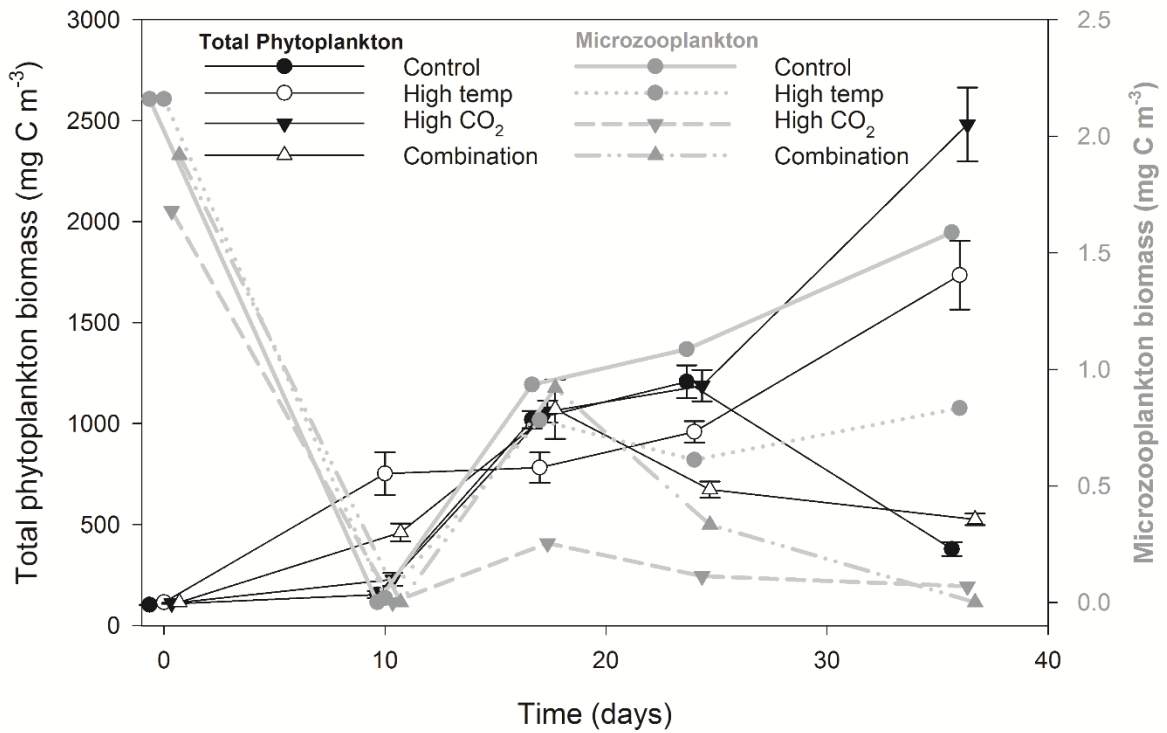


**Fig. 6.** Microzooplankton biomass (dominated by *Strombolidium* sp.) relative to total phytoplankton biomass.

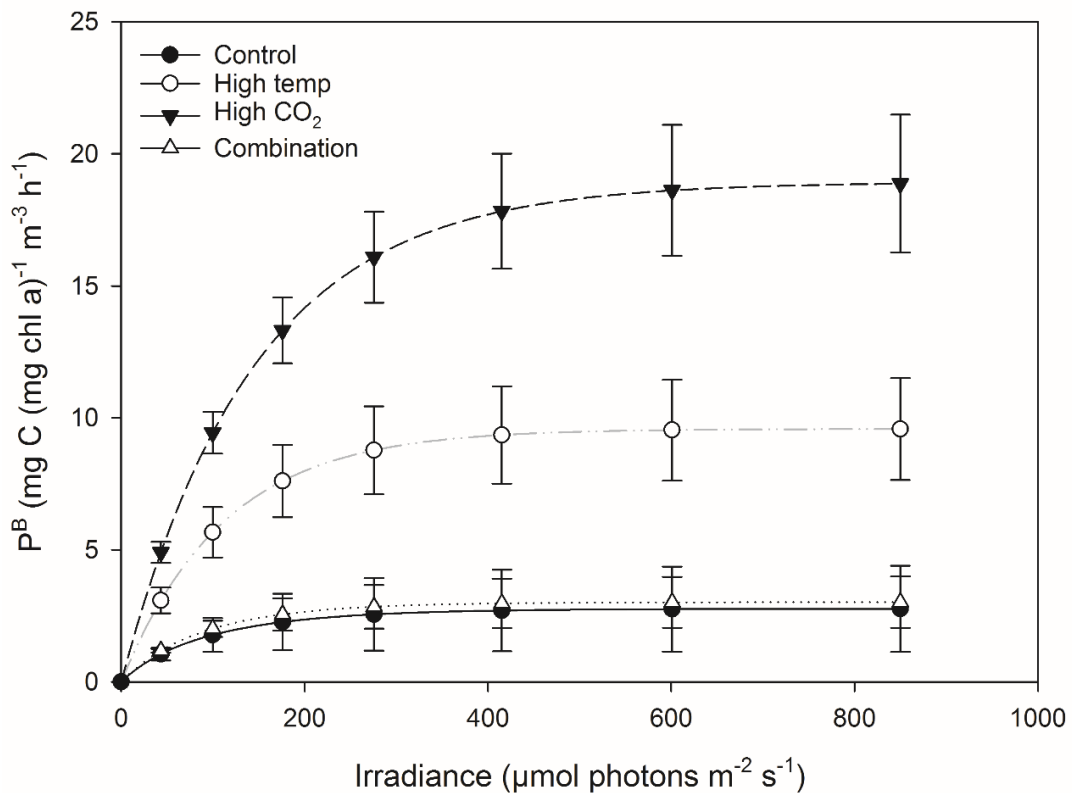


**Fig. 7.** Fitted parameters of FRRf-based photosynthesis-irradiance curves for the experimental treatments on the final experimental day (T36)

944  
945  
946

**Table 1.** Results of generalized linear mixed model testing for effects of time, temperature, pCO<sub>2</sub> and all interactions on chl *a*, phytoplankton biomass and particulate organic carbon and nitrogen. Significant results are in bold; \* p < 0.05, \*\* p < 0.01, \*\*\* p < 0.001.

<b>Response variable</b>	<b>n</b>	<b>df</b>	<b>z-value</b>	<b>p</b>	<b>sig</b>
<b><u>Chla (mg m<sup>-3</sup>)</u></b>					
High temp	516	507	0.412	0.680	
High pCO <sub>2</sub>	516	507	0.664	0.507	
Time	516	507	3.815	<b>&lt;0.001</b>	***
High temp x high pCO <sub>2</sub>	516	507	1.100	0.271	
Time x high temp	516	507	-0.213	0.831	
Time x high CO <sub>2</sub>	516	507	-0.011	0.991	
Time x high temp x high CO <sub>2</sub>	516	507	0.340	0.734	
<b><u>Estimated biomass (mg C m<sup>-3</sup>)</u></b>					
High temp	80	71	0.092	0.927	
High pCO <sub>2</sub>	80	71	2.102	<b>0.036</b>	*
Time	80	71	2.524	<b>0.012</b>	*
High temp x high pCO <sub>2</sub>	80	71	1.253	0.210	
Time x high temp	80	71	1.866	0.062	
Time x high CO <sub>2</sub>	80	71	4.414	<b>&lt;0.001</b>	***
Time x high temp x high CO <sub>2</sub>	80	71	-1.050	0.294	
<b><u>POC (mg m<sup>-3</sup>)</u></b>					
High temp	48	38	-0.977	0.328	
High pCO <sub>2</sub>	48	38	-0.866	0.386	
Time	48	38	-0.203	0.839	
High temp x high pCO <sub>2</sub>	48	38	-0.29	0.772	
Time x high temp	48	38	3.648	<b>&lt;0.001</b>	***
Time x high CO <sub>2</sub>	48	38	4.333	<b>&lt;0.001</b>	***
Time x high temp x high CO <sub>2</sub>	48	38	0.913	0.361	
<b><u>PON (mg m<sup>-3</sup>)</u></b>					
High temp	48	38	-0.640	0.522	
High pCO <sub>2</sub>	48	38	-0.479	0.632	
Time	48	38	0.202	0.84	
High temp x high pCO <sub>2</sub>	48	38	0.667	0.505	
Time x high temp	48	38	1.674	0.094	
Time x high CO <sub>2</sub>	48	38	2.037	<b>&lt; 0.05</b>	*
Time x high temp x high CO <sub>2</sub>	48	38	-0.141	0.730	
<b><u>POC:PON μM C:μM N</u></b>					
High temp	48	38	0.394	0.6937	
High pCO <sub>2</sub>	48	38	0.346	0.7295	
Time	48	38	0.184	0.8538	
High temp x high pCO <sub>2</sub>	48	38	0.253	0.8006	
Time x high temp	48	38	-2.035	<b>0.0418</b>	*
Time x high CO <sub>2</sub>	48	38	-2.445	<b>0.0145</b>	*
Time x high temp x high CO <sub>2</sub>	48	38	-0.673	0.5007	

947

948  
949  
950

**Table 2.** Results of generalized linear mixed model testing for significant effects of time, temperature, pCO<sub>2</sub> and all interactions on phytoplankton species biomass. Significant results are in bold;

\* p < 0.05, \*\* p < 0.01, \*\*\* p < 0.001.

<b>Response variable</b>	<b>n</b>	<b>df</b>	<b>z-value</b>	<b>p</b>	<b>sig</b>
<b>Diatoms (mg C m<sup>-3</sup>)</b>					
High temp	80	70	-0.216	0.829	
High pCO <sub>2</sub>	80	70	-0.895	0.371	
Time	80	70	2.951	<b>0.003</b>	<b>**</b>
High temp x high pCO <sub>2</sub>	80	70	1.063	0.288	
Time x high temp	80	70	-1.151	0.250	
Time x high CO <sub>2</sub>	80	70	0.560	0.576	
Time x high temp x high CO <sub>2</sub>	80	70	0.368	0.713	
<b>Dinoflagellates (mg C m<sup>-3</sup>)</b>					
High temp	80	70	-0.018	0.986	
High pCO <sub>2</sub>	80	70	0.487	0.627	
Time	80	70	-2.347	<b>0.019</b>	<b>*</b>
High temp x high pCO <sub>2</sub>	80	70	-0.166	0.868	
Time x high temp	80	70	1.857	0.063	
Time x high CO <sub>2</sub>	80	70	1.009	0.313	
Time x high temp x high CO <sub>2</sub>	80	70	2.207	<b>0.027</b>	<b>*</b>
<b>Nanophytoplankton (mg m<sup>-3</sup>)</b>					
High temp	80	70	-0.371	0.710	
High pCO <sub>2</sub>	80	70	-2.108	<b>0.035</b>	<b>*</b>
Time	80	70	2.162	<b>0.031</b>	<b>*</b>
High temp x high pCO <sub>2</sub>	80	70	0.79	0.430	
Time x high temp	80	70	1.695	0.090	
Time x high CO <sub>2</sub>	80	70	3.563	<b>&lt;0.001</b>	<b>***</b>
Time x high temp x high CO <sub>2</sub>	80	70	-0.806	0.420	
<b>Synechococcus (mg m<sup>-3</sup>)</b>					
High temp	80	70	3.333	<b>&lt;0.001</b>	<b>***</b>
High pCO <sub>2</sub>	80	70	2.231	<b>0.026</b>	<b>*</b>
Time	80	70	0.049	0.961	
High temp x high pCO <sub>2</sub>	80	70	2.391	<b>0.017</b>	<b>*</b>
Time x high temp	80	70	4.076	<b>&lt;0.001</b>	<b>***</b>
Time x high CO <sub>2</sub>	80	70	-1.553	0.1204	
Time x high temp x high CO <sub>2</sub>	80	70	5.382	<b>&lt;0.001</b>	<b>***</b>
<b>Picophytoplankton (mg m<sup>-3</sup>)</b>					
High temp	80	70	0.951	0.342	
High pCO <sub>2</sub>	80	70	-0.472	0.637	
Time	80	70	0.897	0.370	
High temp x high pCO <sub>2</sub>	80	70	-1.188	0.235	
Time x high temp	80	70	-0.219	0.827	
Time x high CO <sub>2</sub>	80	70	1.411	0.158	
Time x high temp x high CO <sub>2</sub>	80	70	2.792	<b>0.005</b>	<b>**</b>
<b>Coccolithophores (mg C m<sup>-3</sup>)</b>					
High temp	80	70	-0.408	0.683	
High pCO <sub>2</sub>	80	70	-0.308	0.758	
Time	80	70	0.211	0.833	
High temp x high pCO <sub>2</sub>	80	70	-0.319	0.750	

**Table 2 cont'd**

Time x high temp	80	70	0.269	0.788	
Time x high CO <sub>2</sub>	80	70	0.295	0.768	
Time x high temp x high CO <sub>2</sub>	80	70	0.502	0.615	
<b>Cryptophytes (mg C m<sup>-3</sup>)</b>					
High temp	80	70	0.207	0.836	
High pCO <sub>2</sub>	80	70	0.256	0.798	
Time	80	70	-5.289	<b>&lt;0.001</b>	<b>***</b>
High temp x high pCO <sub>2</sub>	80	70	-0.349	0.727	
Time x high temp	80	70	1.885	0.059	
Time x high CO <sub>2</sub>	80	70	0.167	0.867	
Time x high temp x high CO <sub>2</sub>	80	70	1.694	0.090	
<b>Microzooplankton (mg C m<sup>-3</sup>)</b>					
High temp	80	70	0.138	0.890	
High pCO <sub>2</sub>	80	70	-0.142	0.887	
Time	80	70	0.418	0.676	
High temp x high pCO <sub>2</sub>	80	70	0.314	0.753	
Time x high temp	80	70	-0.930	0.352	
Time x high CO <sub>2</sub>	80	70	-2.100	<b>0.036</b>	<b>*</b>
Time x high temp x high CO <sub>2</sub>	80	70	-1.996	<b>0.046</b>	<b>*</b>

951

952

953

954

955

956

957

958

959

**Table 3.** FRRf-based photosynthesis-irradiance curve parameters for the experimental treatments on the final day (T36).

Parameter	Control	sd	High temp	sd	High CO <sub>2</sub>	sd	Combination	sd
<b>P<sup>B</sup><sub>m</sub></b>	2.77	1.63	9.58	1.94	18.93	2.65	3.02	0.97
<b>α</b>	0.03	0.01	0.09	0.01	0.13	0.01	0.04	0.00
<b>I<sub>k</sub></b>	85.33	45.47	110.93	6.09	144.13	17.91	86.38	33.06

960

961

962

963

964

965

966

967 **Table 4.** Results of generalised linear model testing for significant effects of temperature, CO<sub>2</sub> and temperature  
 968 x CO<sub>2</sub> on phytoplankton photophysiology at T36; P<sup>B<sub>m</sub></sup> (maximum photosynthetic rates), α (light limited slope)  
 969 and I<sub>k</sub> (light saturated photosynthesis). Significant results are in bold; \* p < 0.05, \*\* p < 0.001, \*\*\* p < 0.0001.

<b>Response variable</b>	<b>n</b>	<b>df</b>	<b>t-value</b>	<b>p</b>	<b>sig</b>
<b><u>P<sup>B<sub>m</sub></sup></u></b>					
High temp	12	8	7.353	< <b>0.0001</b>	<b>***</b>
High pCO <sub>2</sub>	12	8	8.735	< <b>0.0001</b>	<b>***</b>
High temp x high pCO <sub>2</sub>	12	8	-8.519	< <b>0.0001</b>	<b>***</b>
<b><u>α</u></b>					
High temp	12	8	13.03	< <b>0.0001</b>	<b>***</b>
High pCO <sub>2</sub>	12	8	15.15	< <b>0.0001</b>	<b>***</b>
High temp x high pCO <sub>2</sub>	12	8	-14.82	< <b>0.0001</b>	<b>***</b>
<b><u>I<sub>k</sub></u></b>					
High temp	12	8	2.018	0.0783	
High pCO <sub>2</sub>	12	8	2.541	<b>0.0347</b>	<b>*</b>
High temp x high pCO <sub>2</sub>	12	8	-2.441	<b>0.0405</b>	<b>*</b>

970

971

972